

« Propriétés et évolution des galaxies »

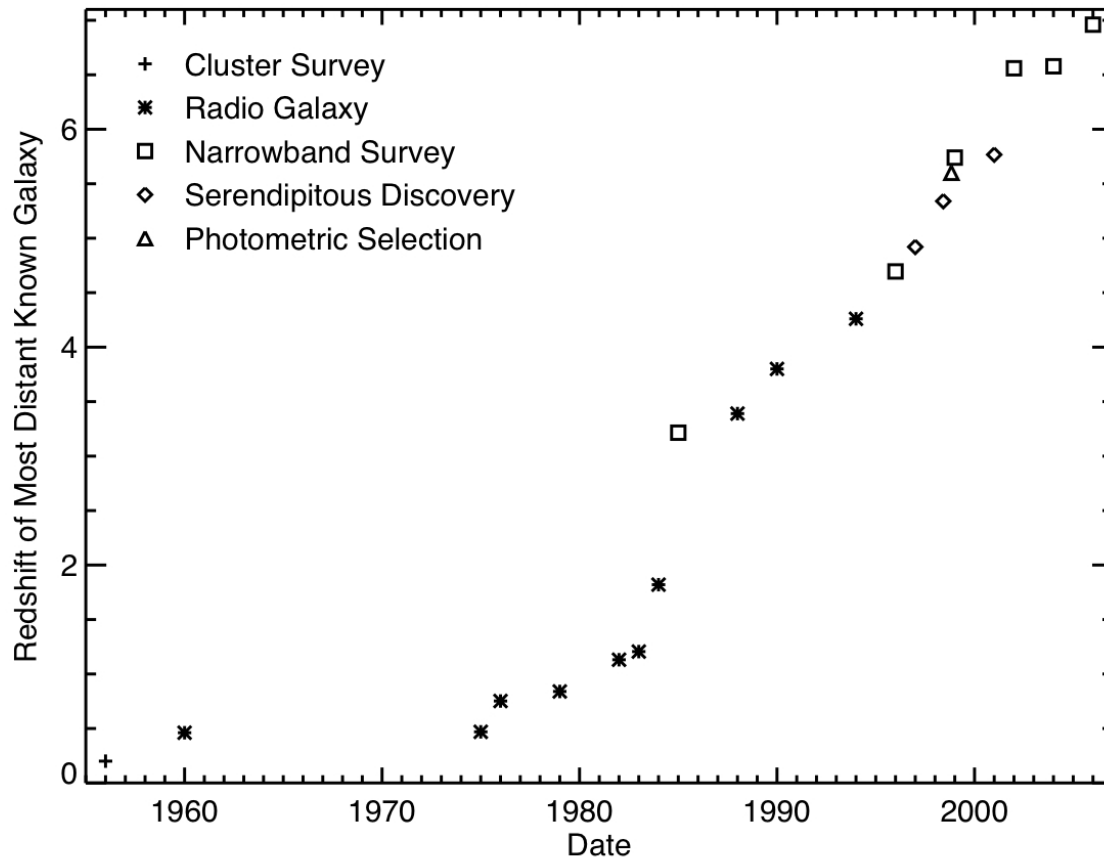
David Elbaz (delbaz@cea.fr)

Service d'Astrophysique - CEA Saclay
Tel: 01 69 08 54 39

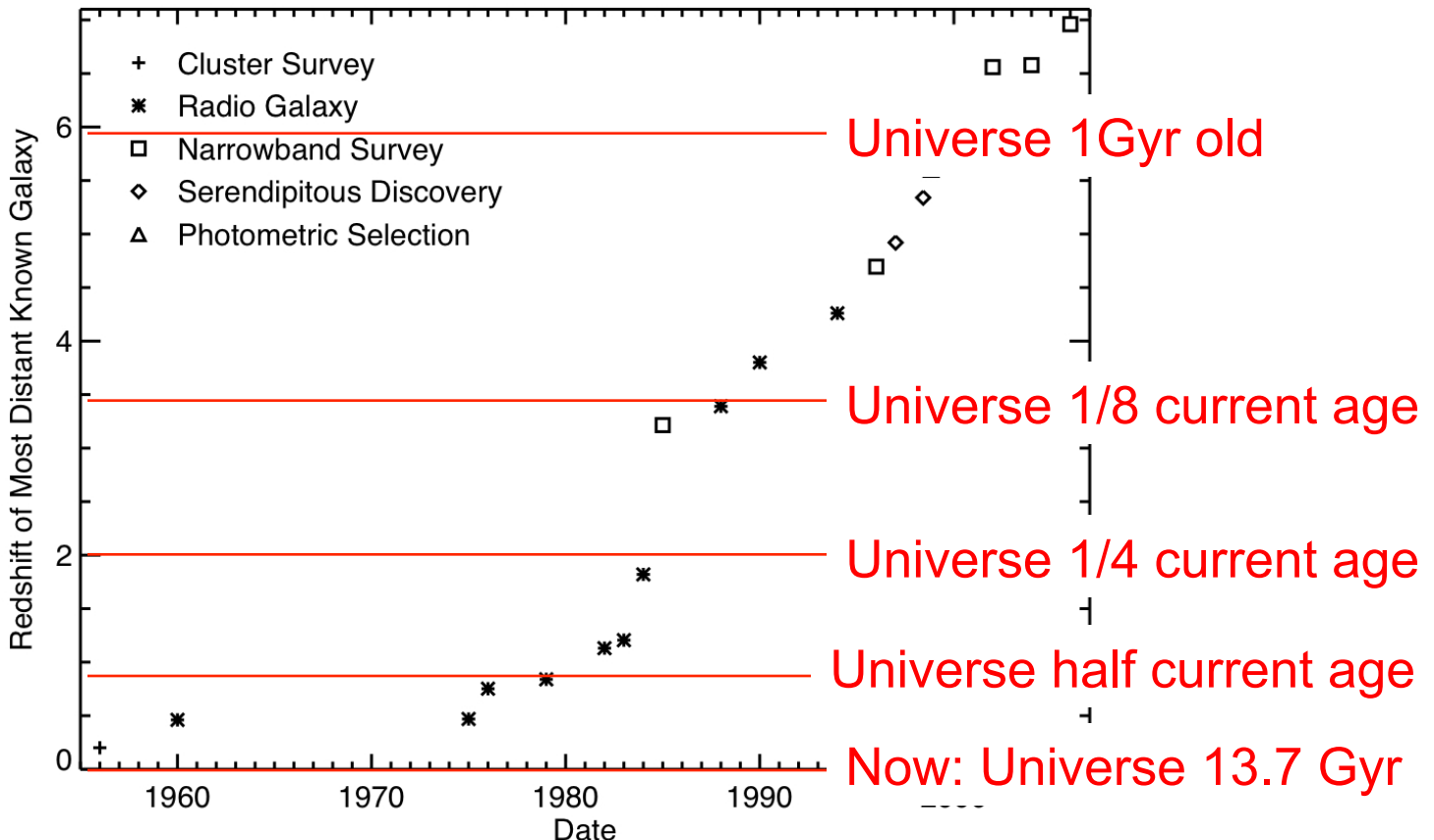
À la recherche des galaxies les plus distantes

Master Recherche M2 Astronomie & Astrophysique
Enseignement thématique des parcours M2 – Galaxies
http://david.elbaz3.free.fr/master_m2

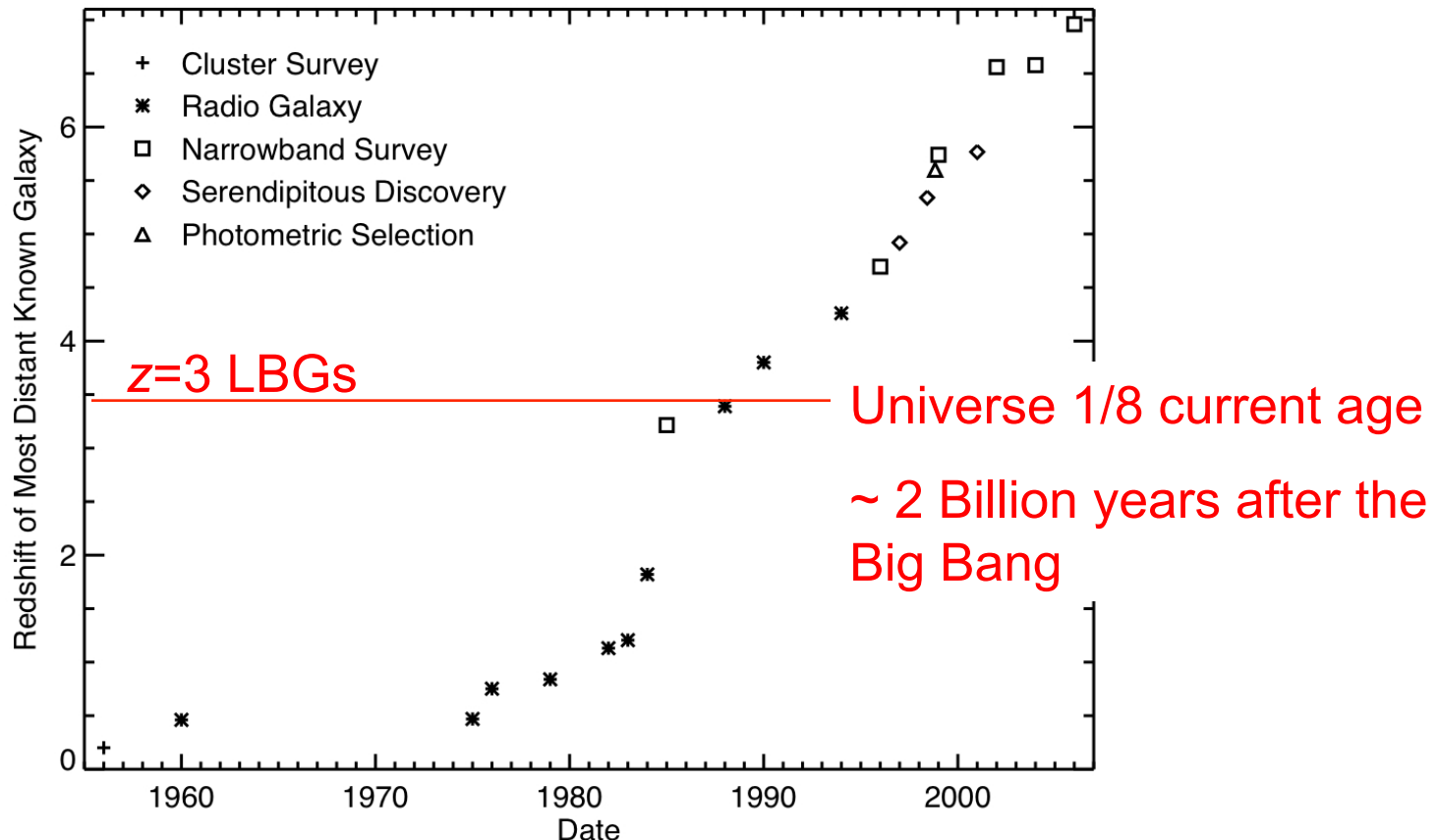
À la recherche de la galaxie la plus distante



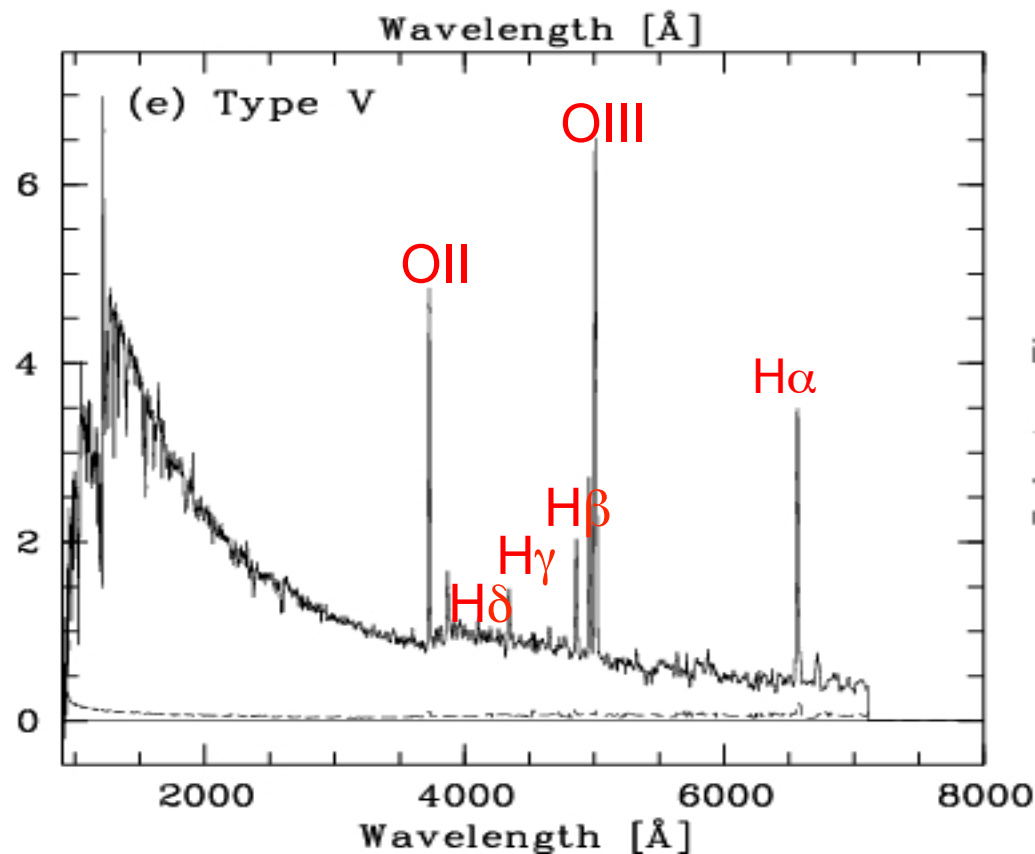
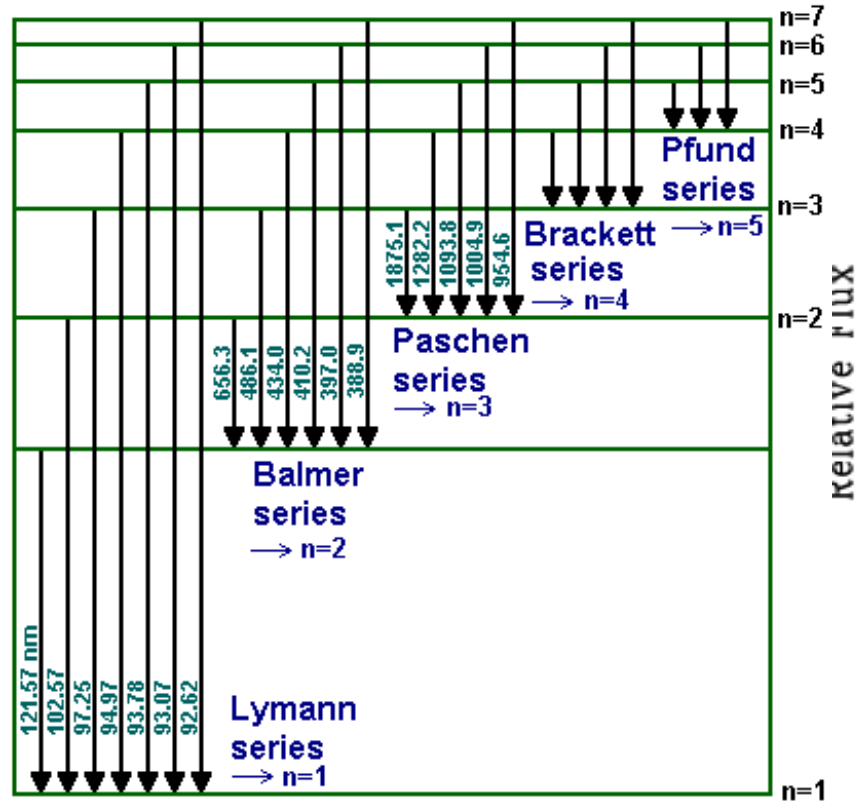
À la recherche de la galaxie la plus distante



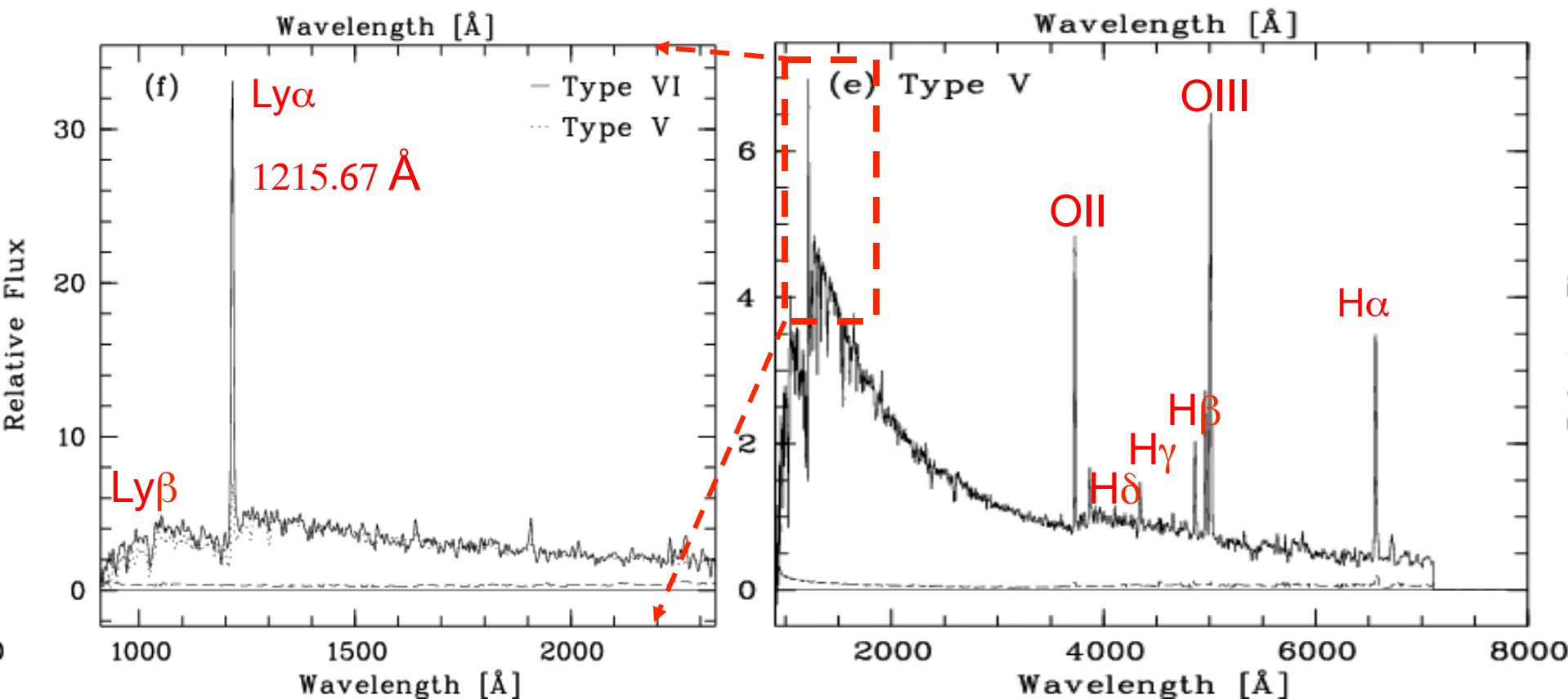
À la recherche de la galaxie la plus distante



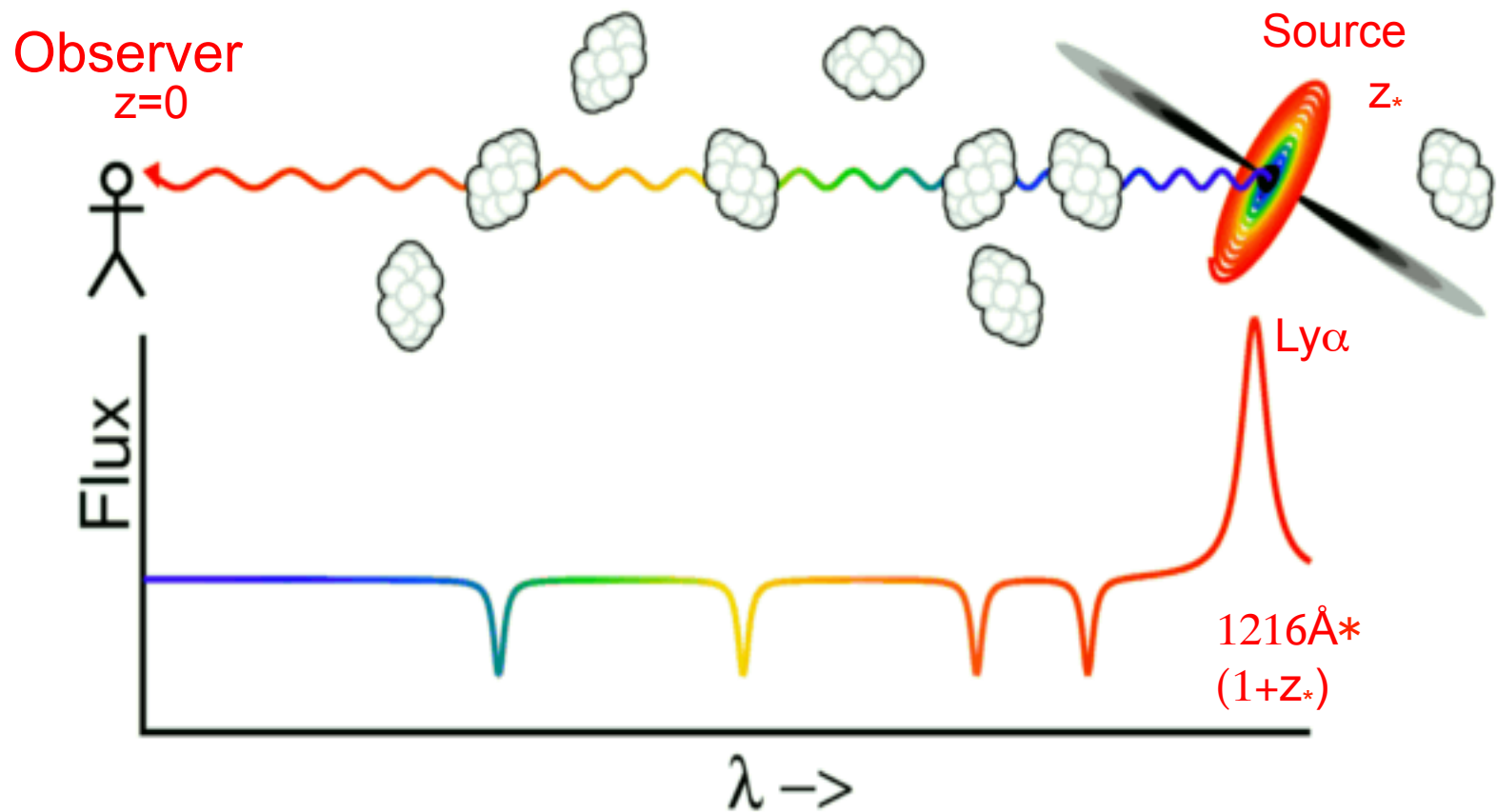
Les raies de Balmer, de Lyman et de l'oxygène pour mesurer le redshift



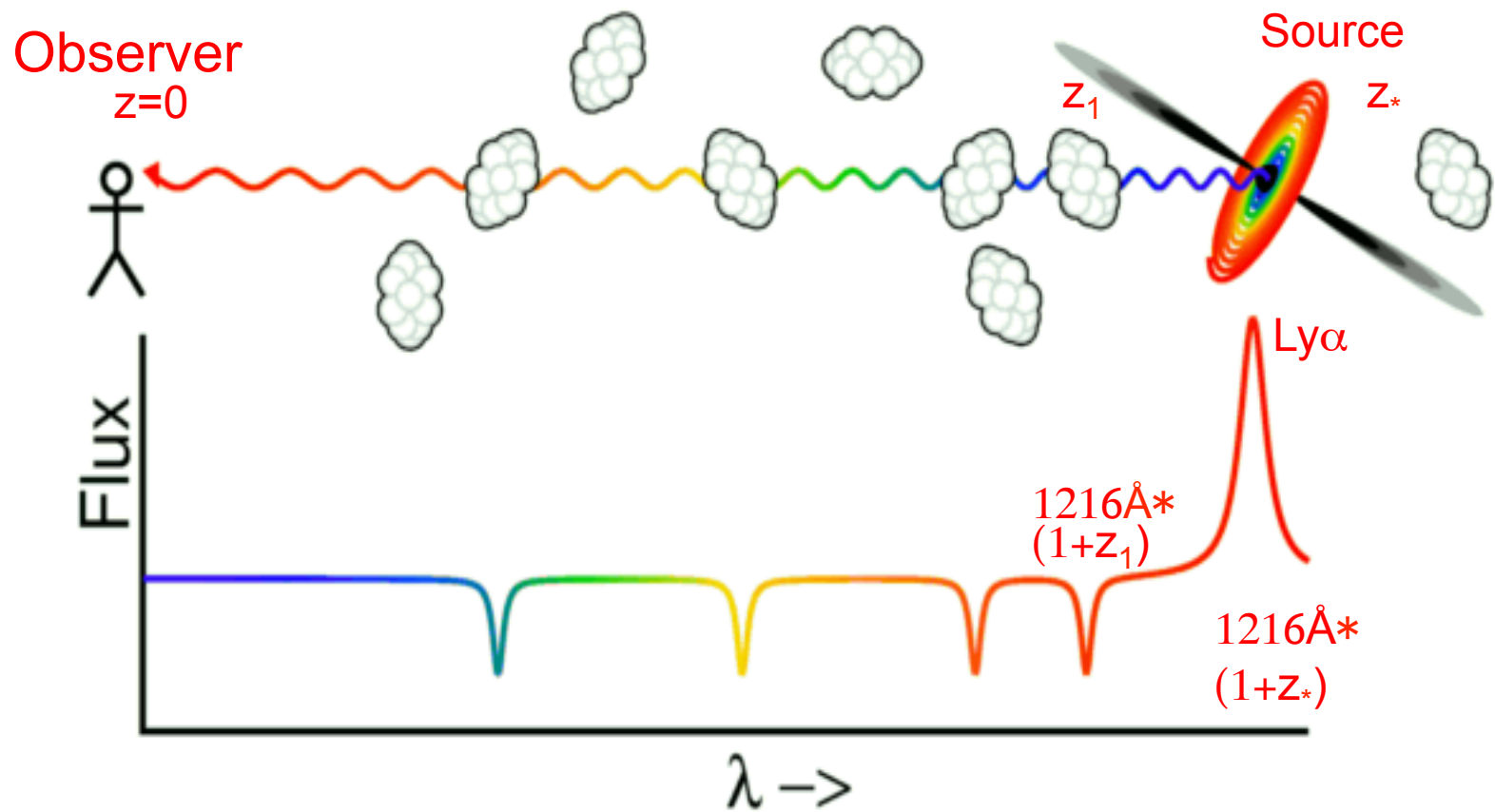
Les raies de Balmer, de Lyman et de l'oxygène pour mesurer le redshift



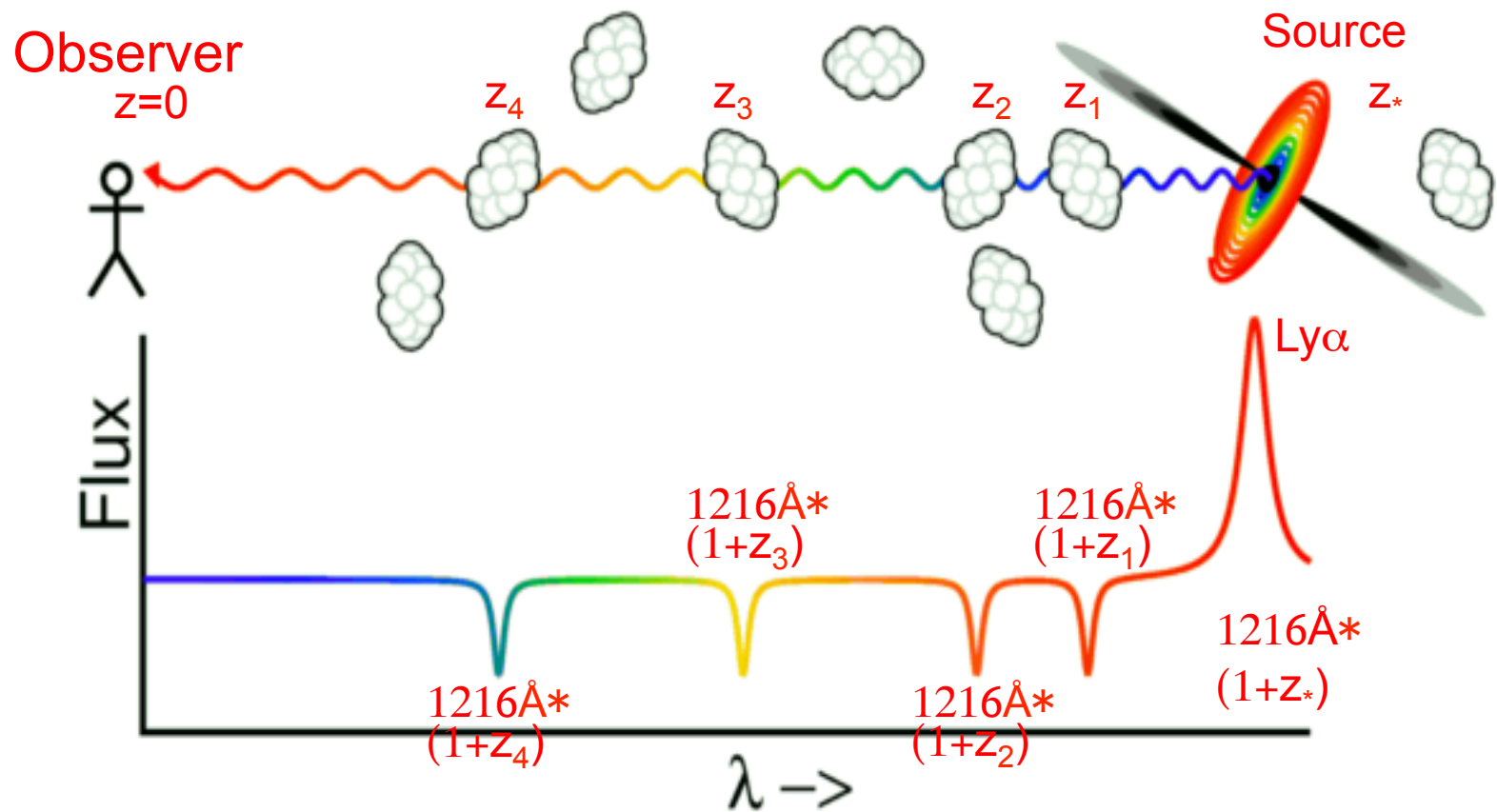
La forêt Lyman α



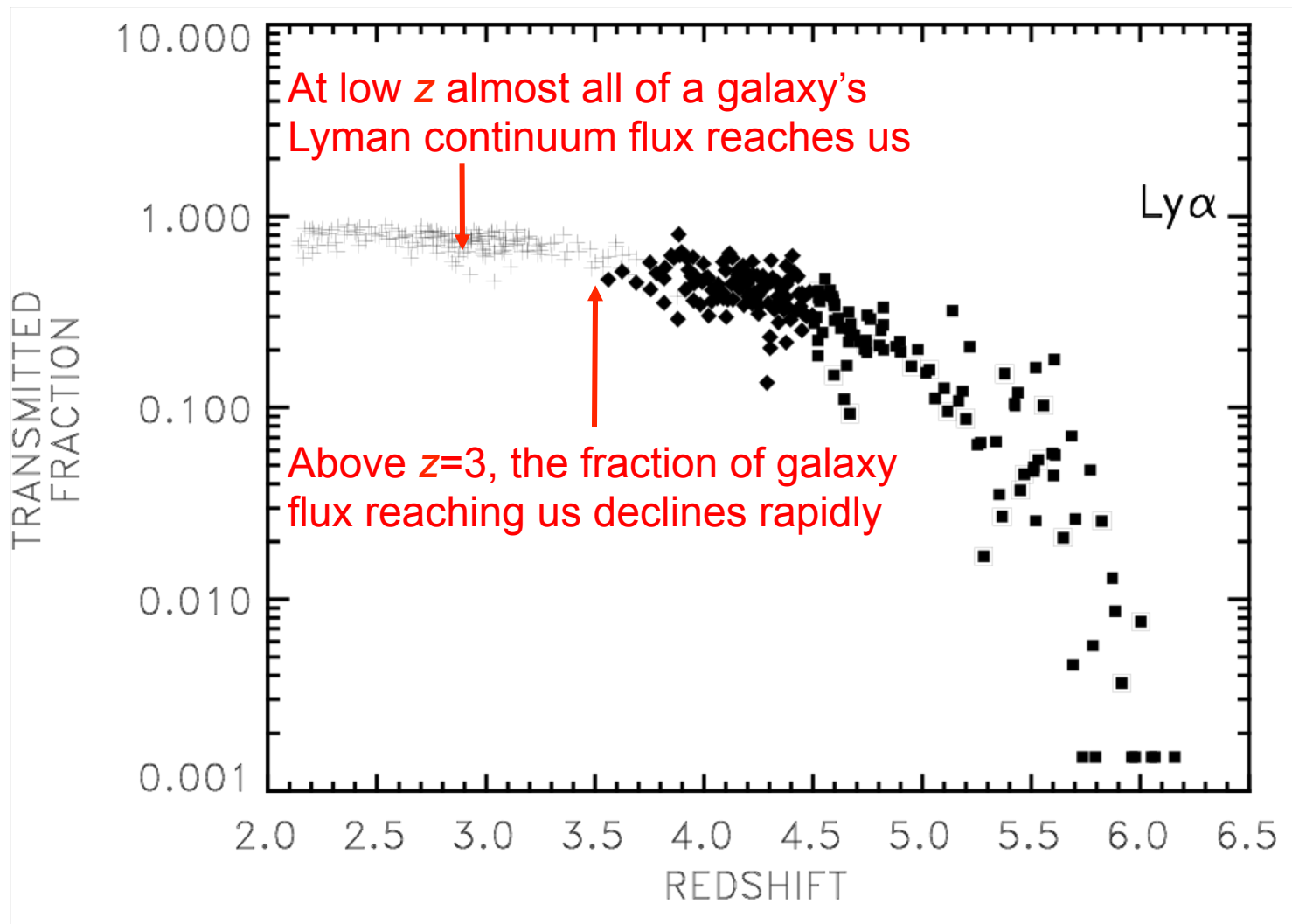
La forêt Lyman α



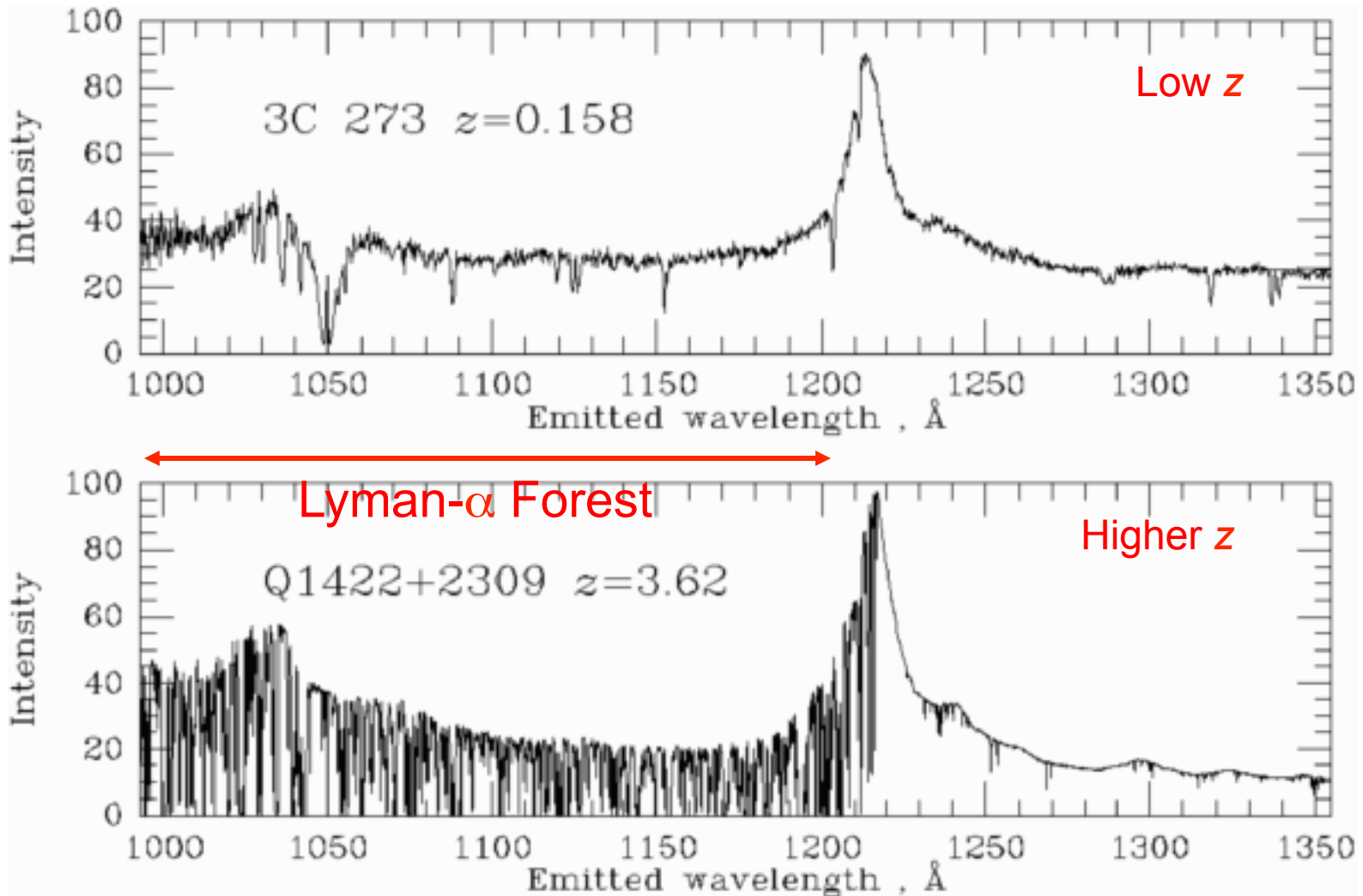
La forêt Lyman α



The Lyman- α Forest

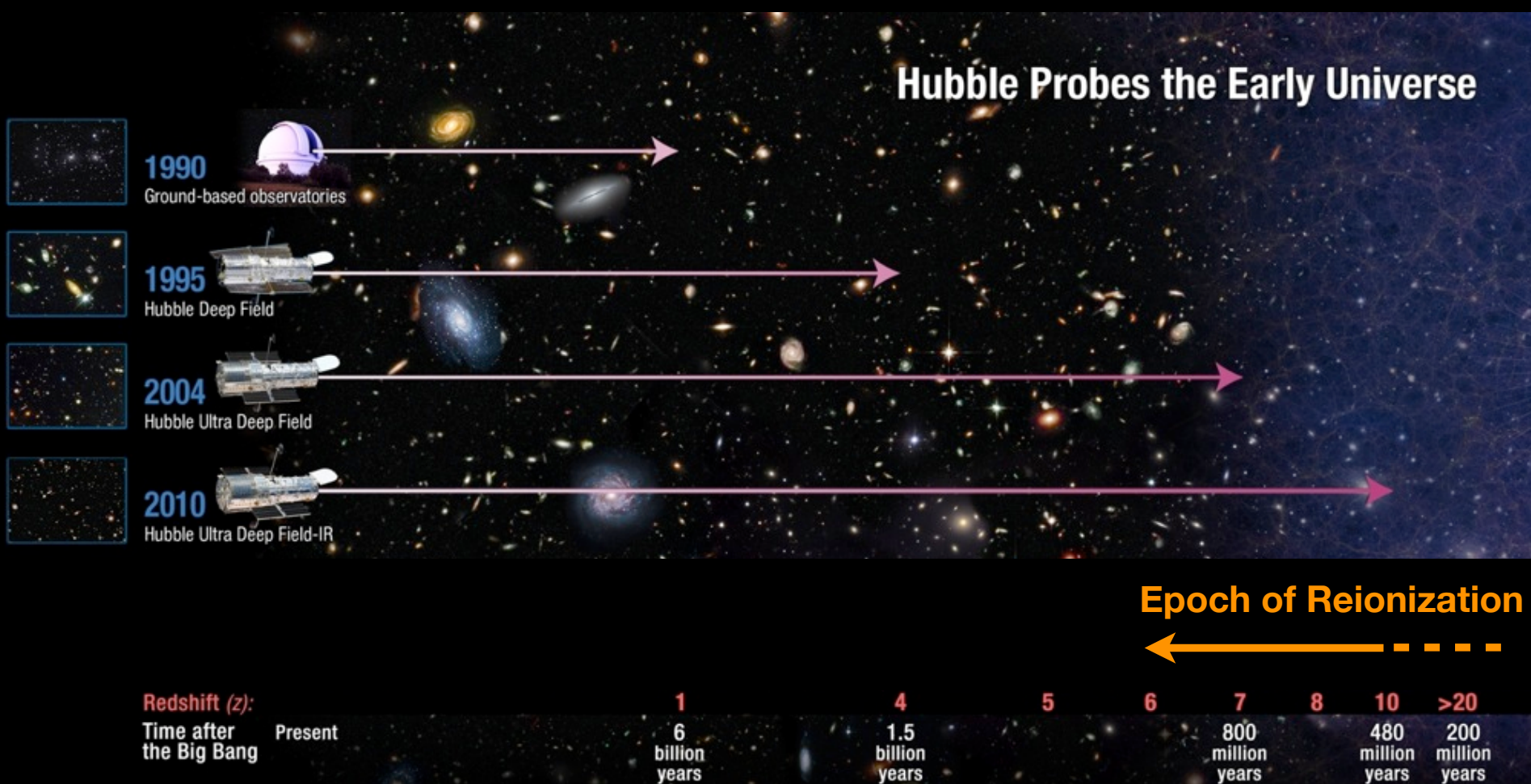


The Lyman- α Forest



The history of astronomy is a history of receding horizons.

E. P. Hubble



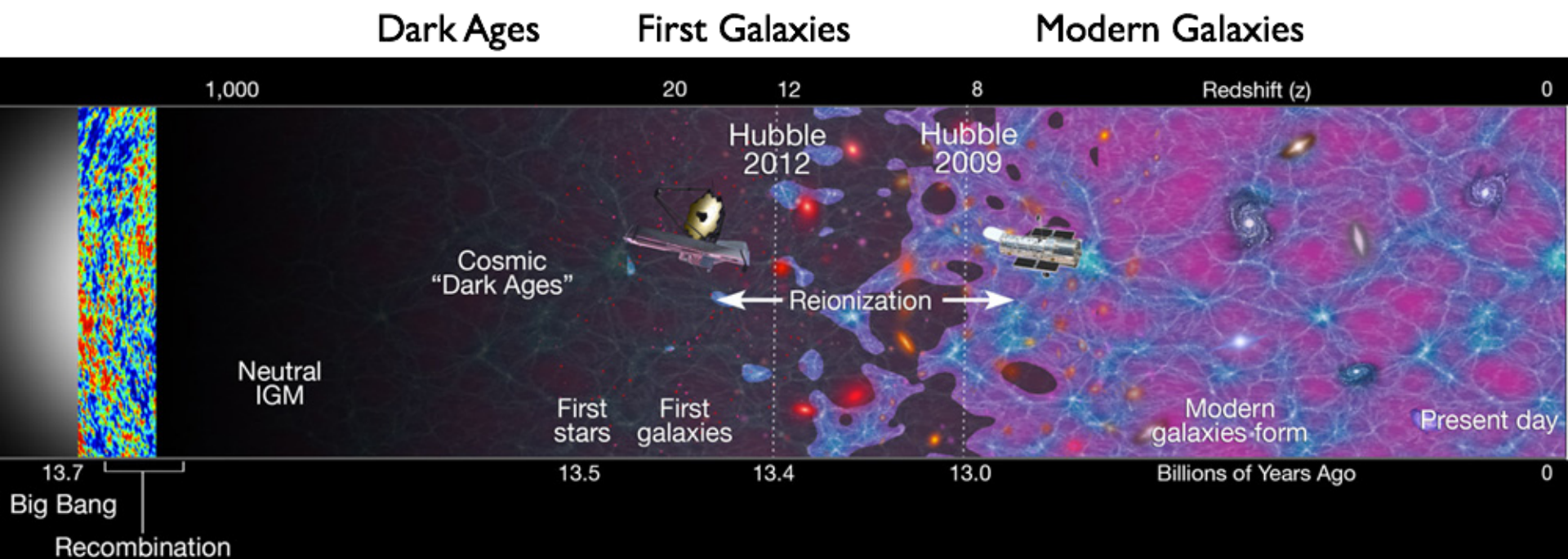
Why are High-Redshift Galaxies Interesting?

Epoch where galaxies were born and rapidly grew...

Epoch where their dark matter halos were assembled

Epoch when the Universe was Reionized...

Did ionizing photons from galaxies drive cosmic reionization?

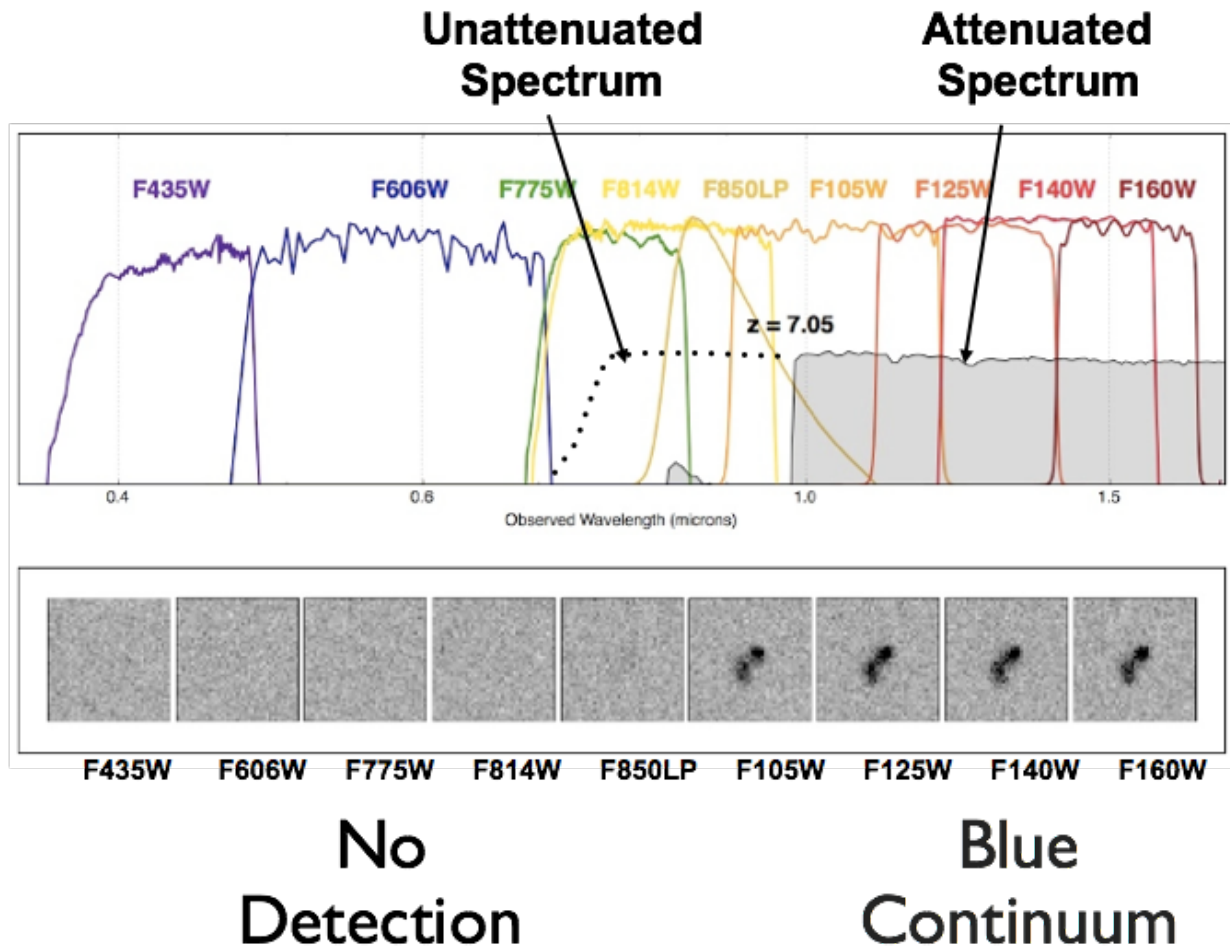


How do we identify galaxies in the early universe?

Lyman Break
Technique

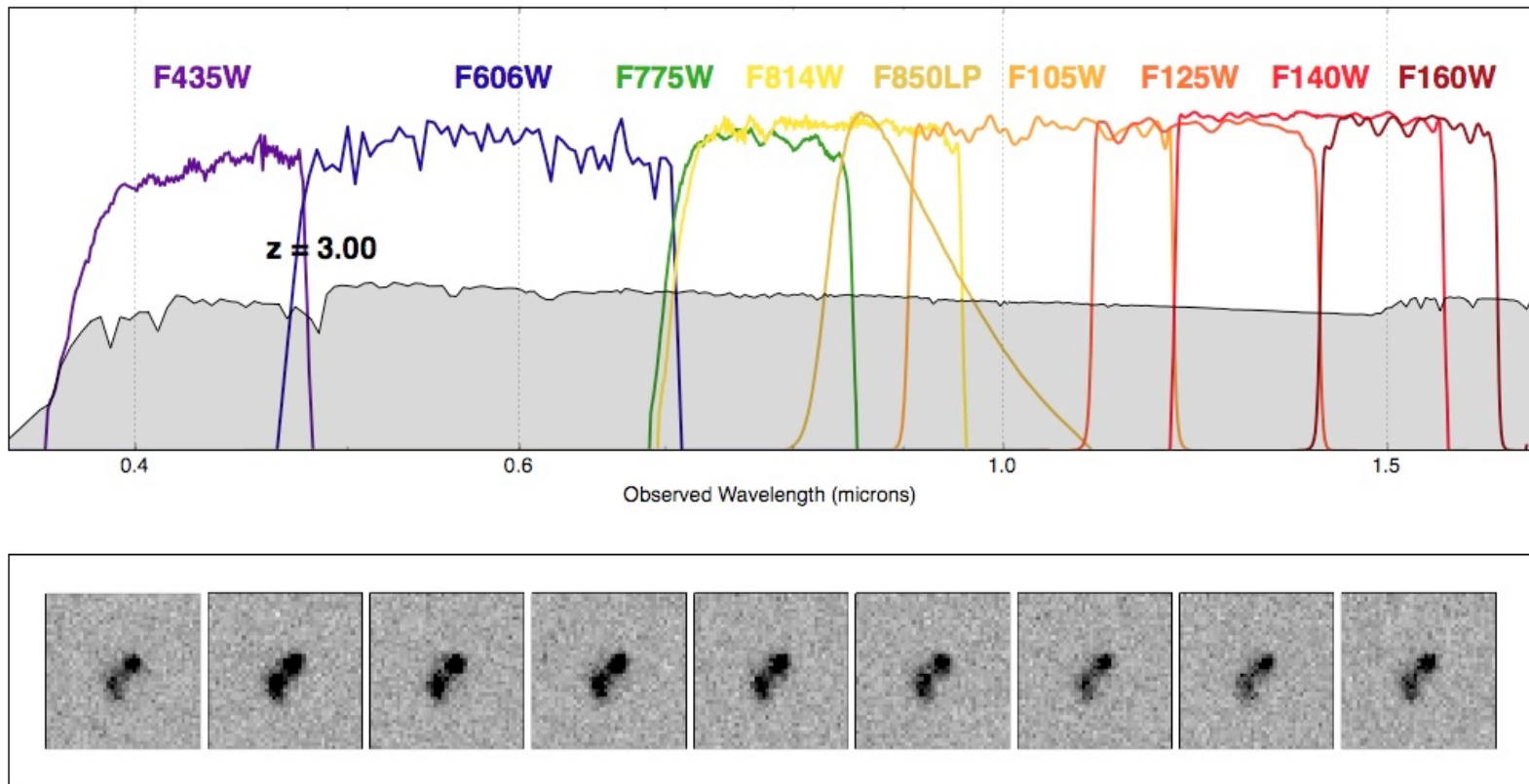
Position of break
tells us the
redshift

Example
 $z=7$ galaxy



How do we identify galaxies in the early universe?

Similar technique works in finding galaxies at $z > 3$:
(strong Spectral Break in otherwise blue source)

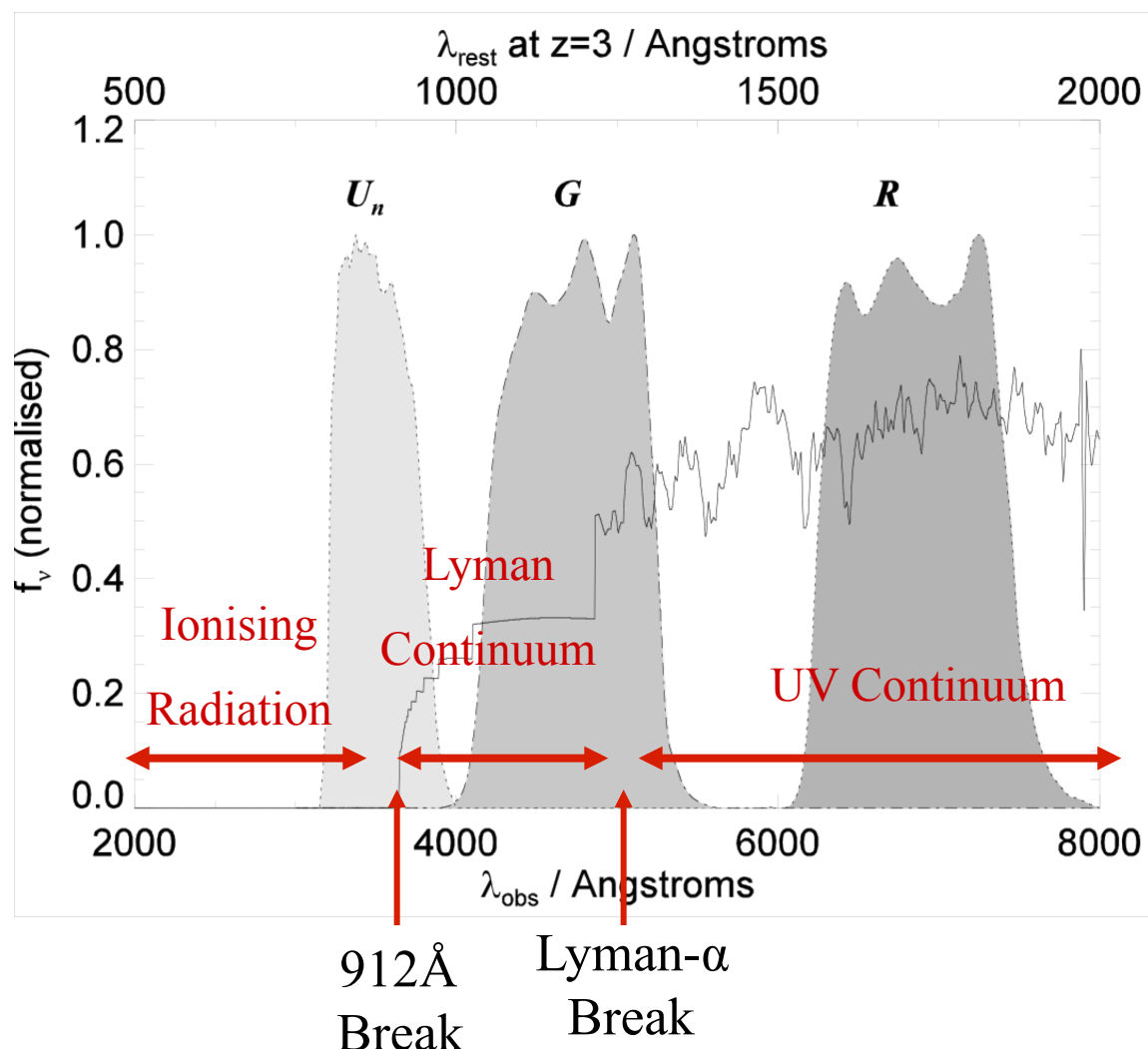


Animation available at <http://xdf.ucolick.org/>

The Lyman Break Technique

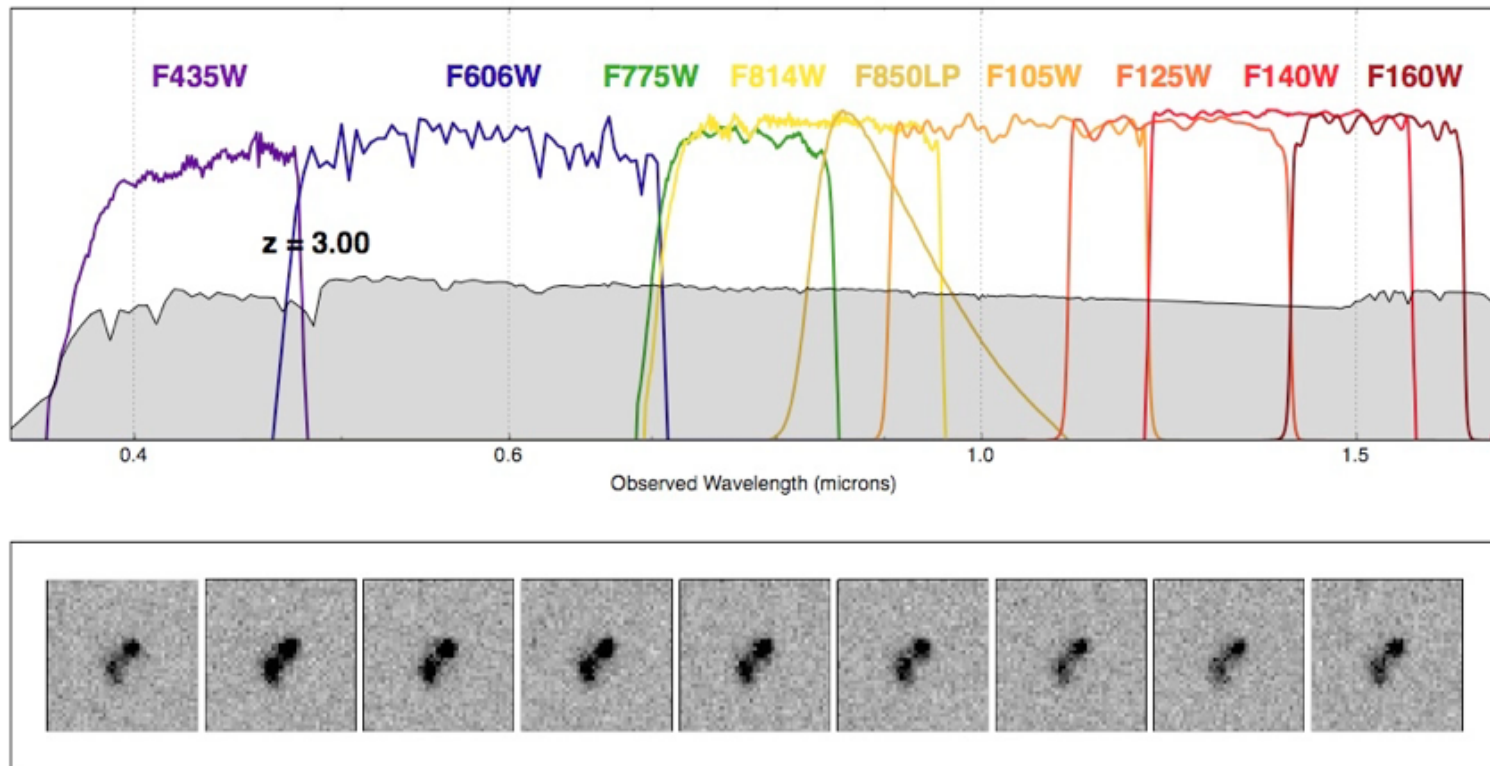
The Steidel, Pettini & Hamilton (1995) Lyman Break Method

- At $z=3$, about 50% of the Lyman continuum is transmitted
- This leads to a ‘break’ in the spectrum



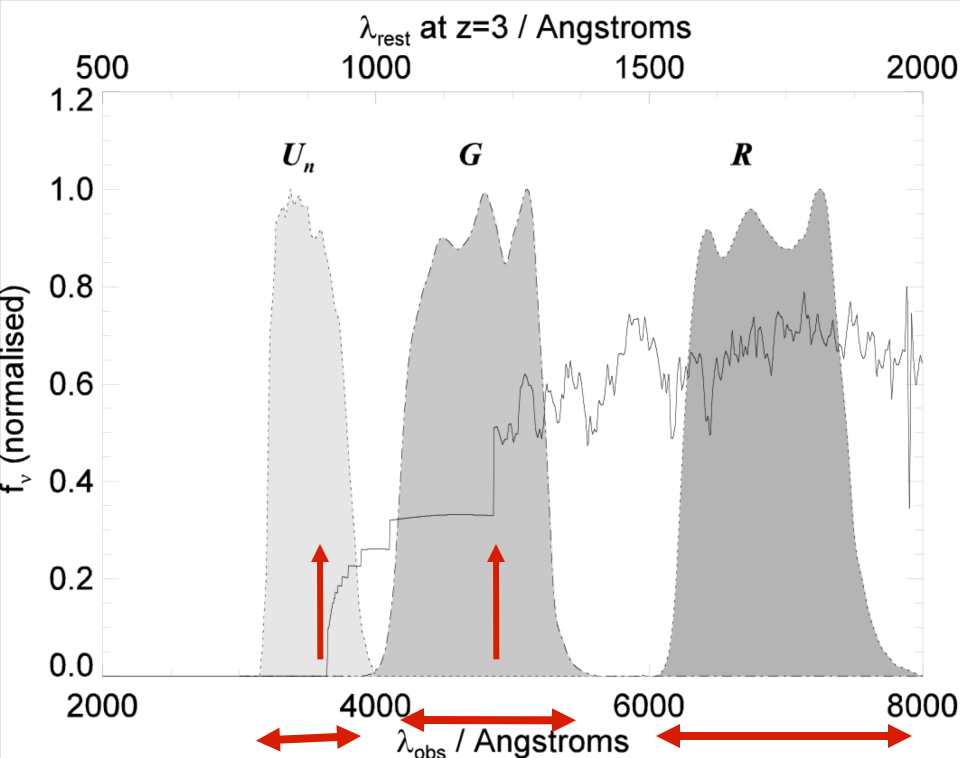
How do we identify galaxies in the early universe?

Similar technique works in finding galaxies at $z > 3$:
(strong Spectral Break in otherwise blue source)

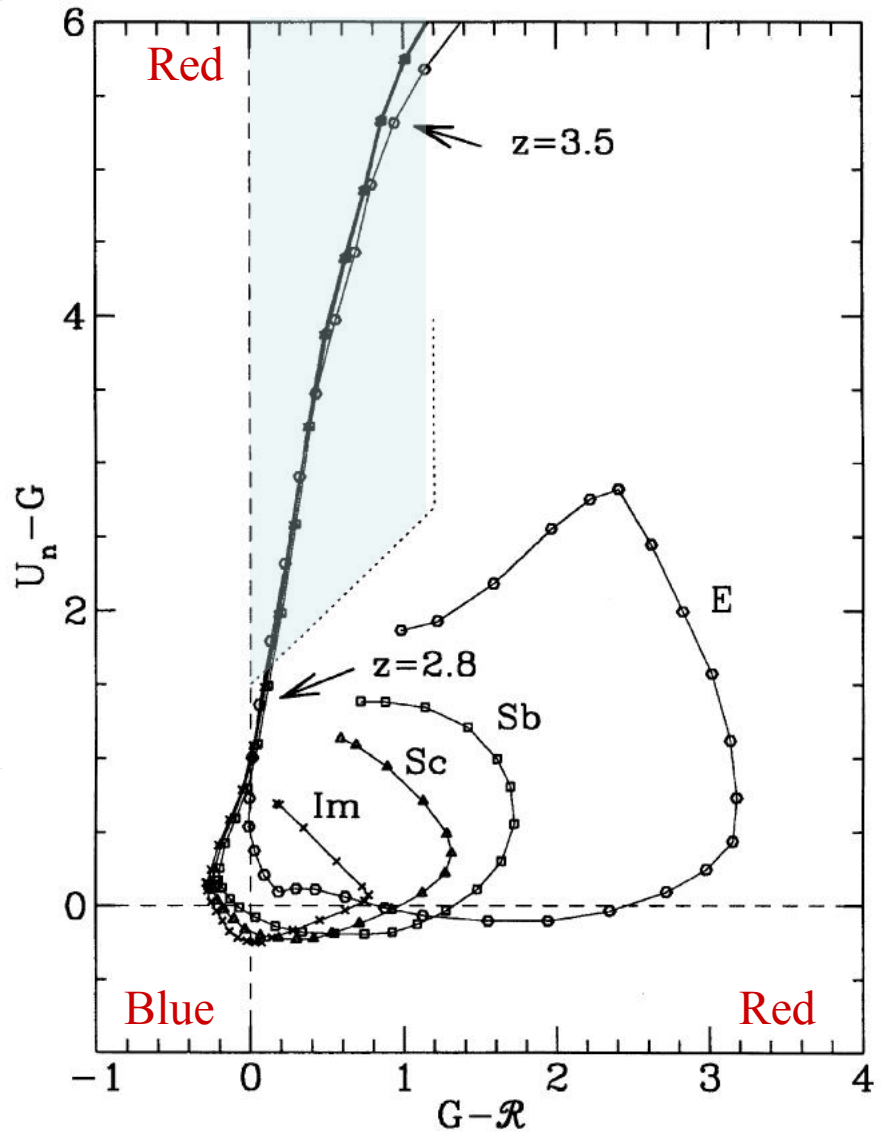


Animation available at <http://xdf.ucolick.org/>

The Lyman Break Technique

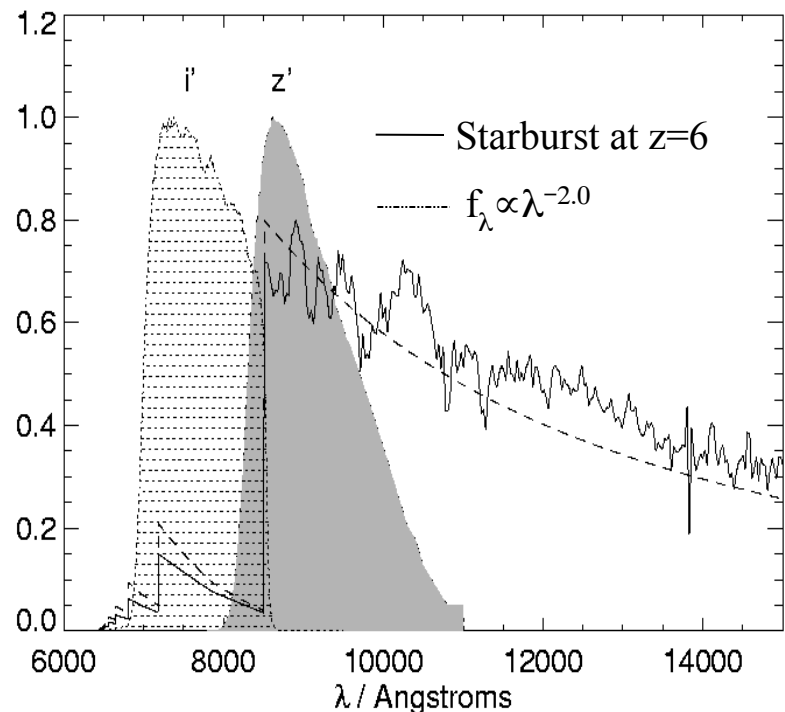


If the filters bracket the breaks, then the galaxies show extreme colours



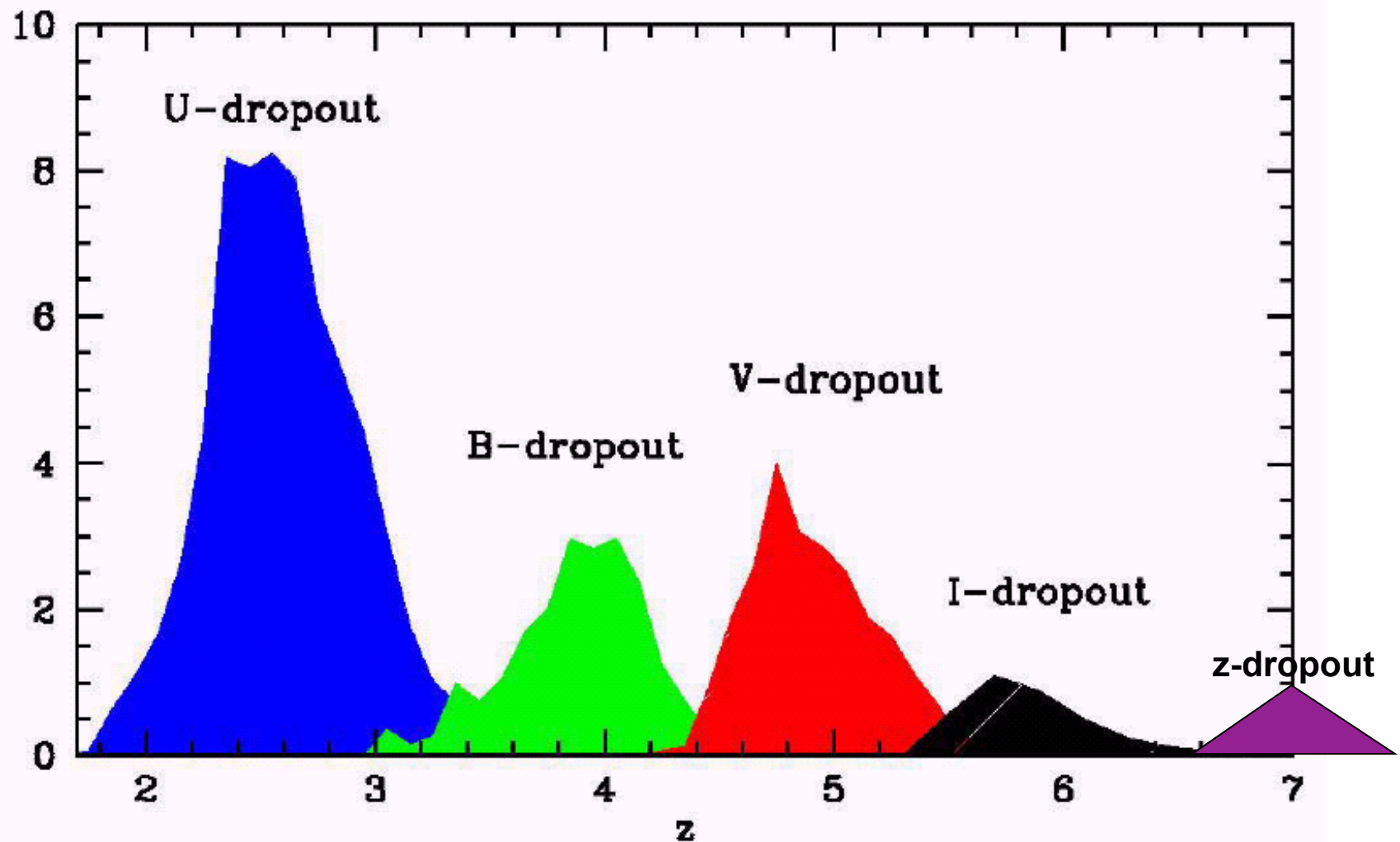
The Dropout Technique

- At $z > 4$, the Lyman forest absorption reaches near 100% \Rightarrow only one break is detected
- A source will be detected in filters above the break but ‘drop-out’ of filters below it
- V-drops $\Rightarrow z > 4.5$
- R-drops $\Rightarrow z > 5.$
- I-drops $\Rightarrow z > 5.8$



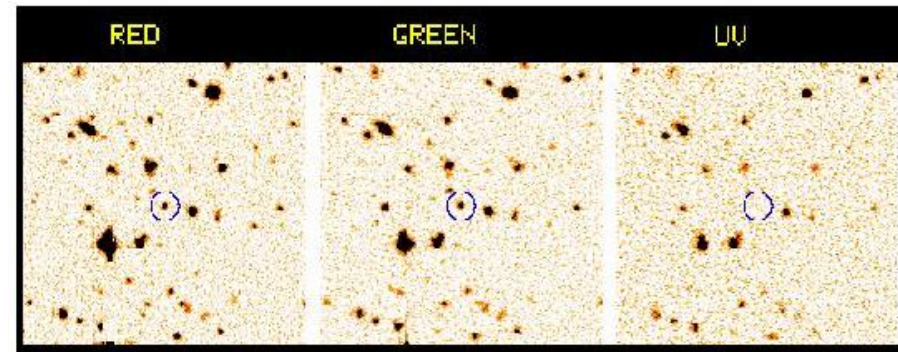
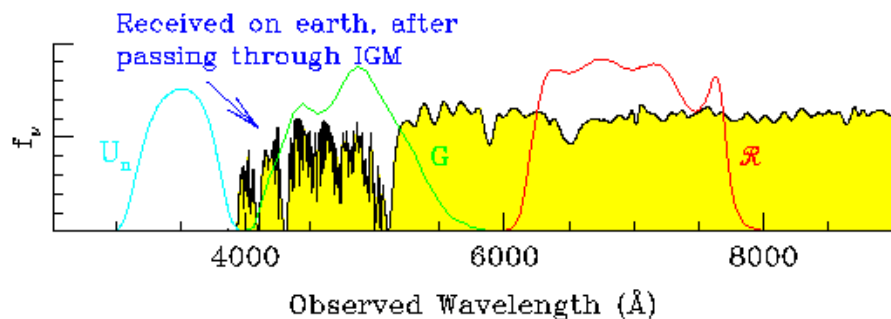
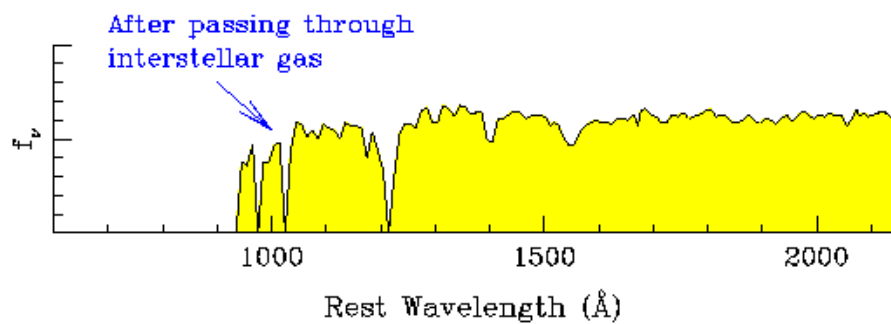
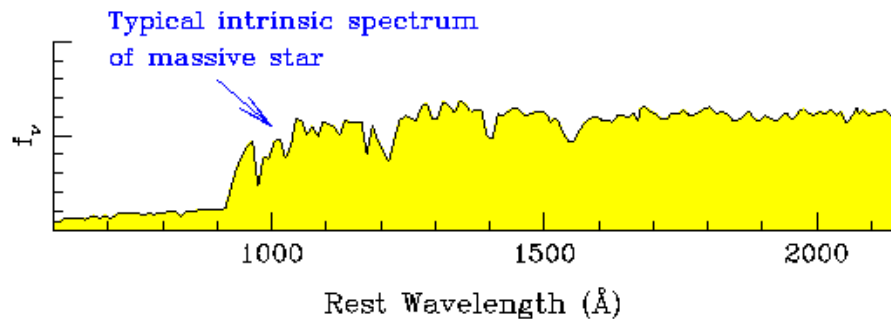
For galaxies at $5.6 < z < 7.0$, $i' - z' > 1.3$

Lyman breaks or 'dropouts' at higher z



Lyman Break Galaxies

Effect of neutral hydrogen



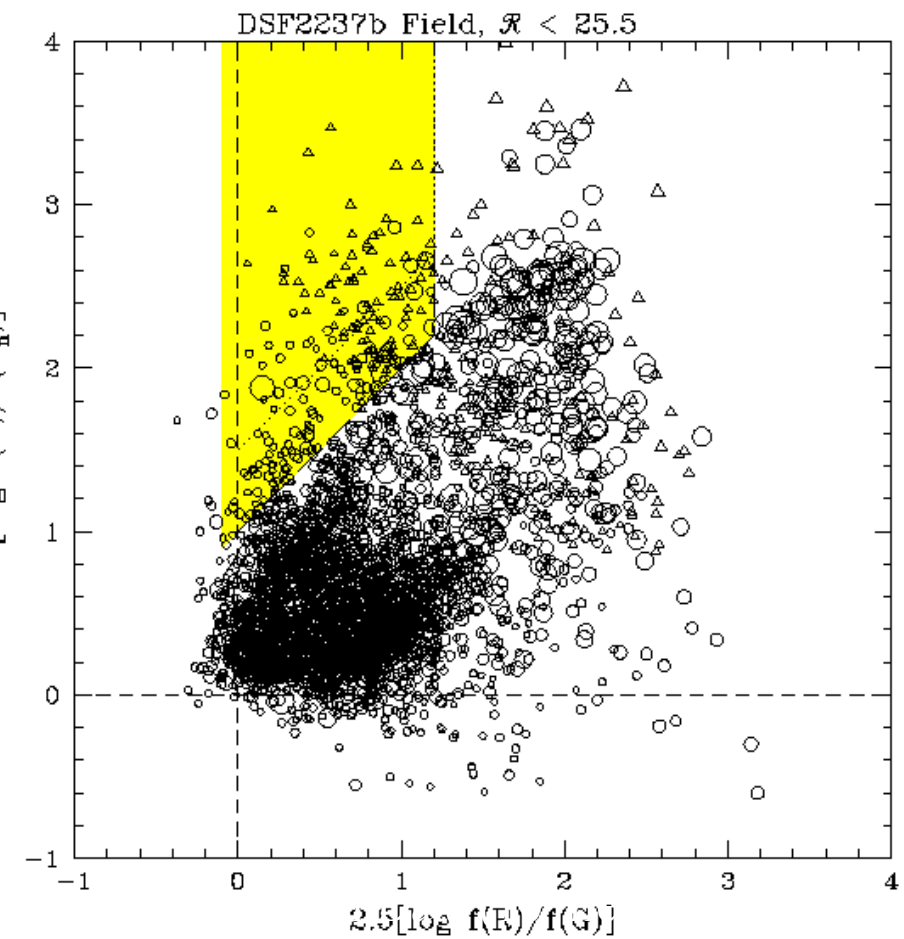
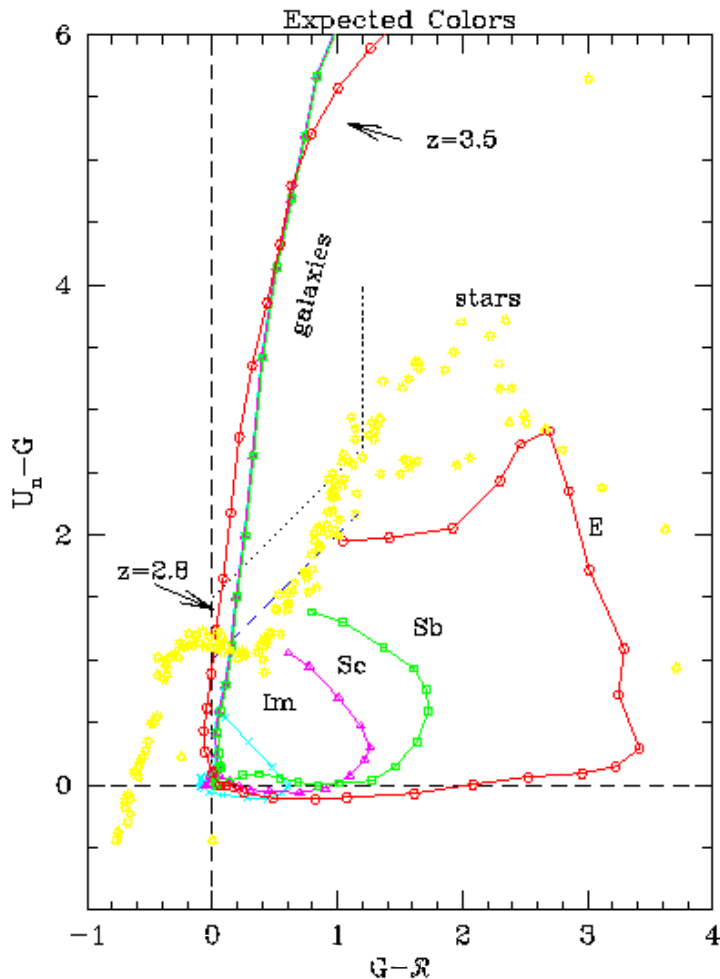
The Lyman continuum discontinuity is particularly powerful for isolating star-forming high redshift galaxies.

From the ground, we have access to the redshift range $z=2.5-6$ in the 0.3-1 micron range.

Steidel et al 1999 Ap J 462, L17
Steidel et al 1999 Ap J 519, 1

Steidel et al 2003 Ap J 592 728

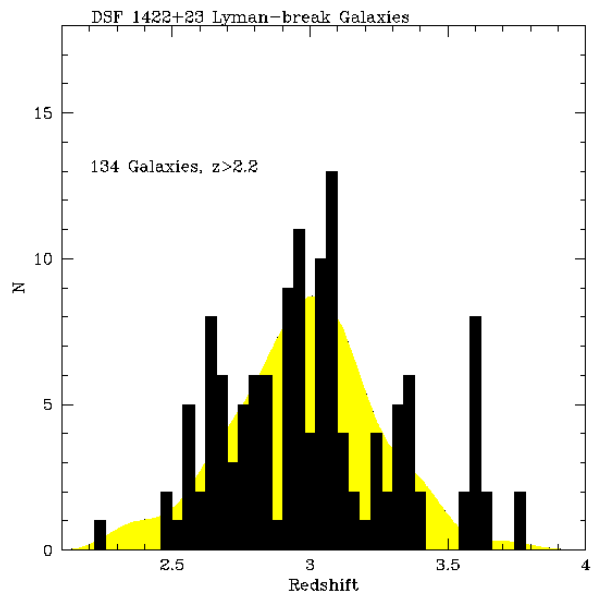
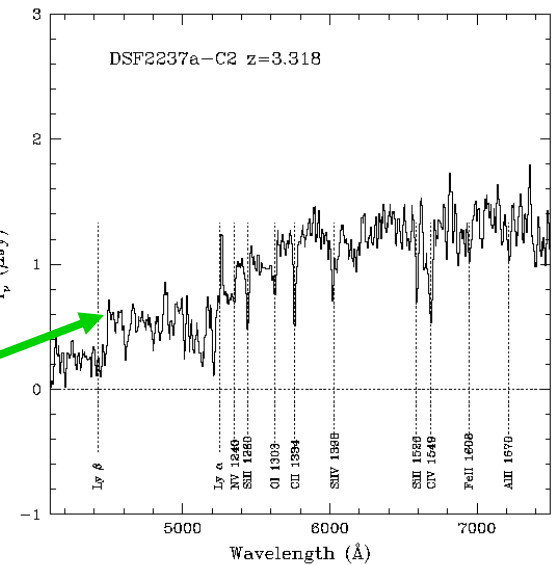
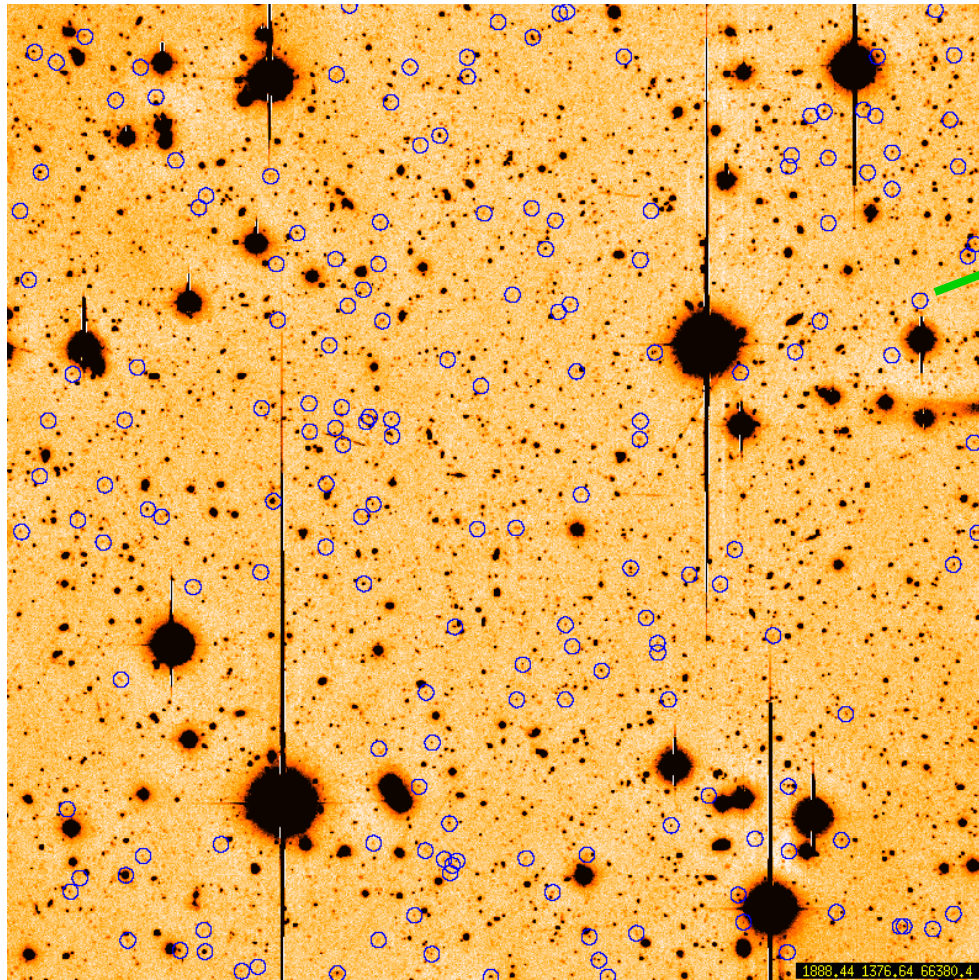
Photometric Cuts: Predictions and Practice



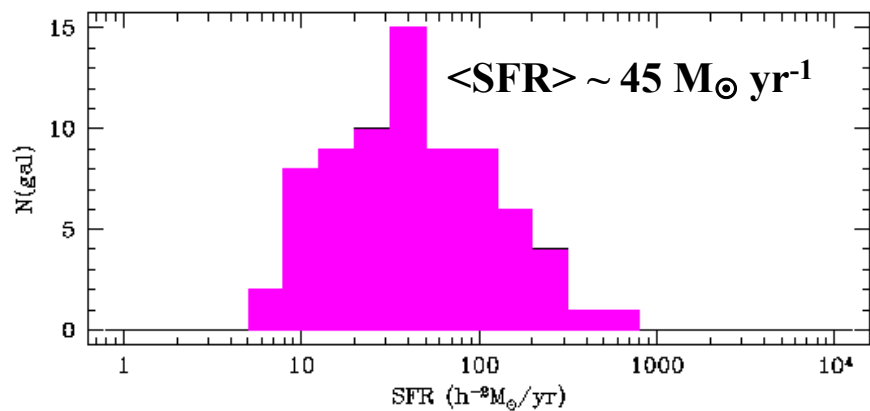
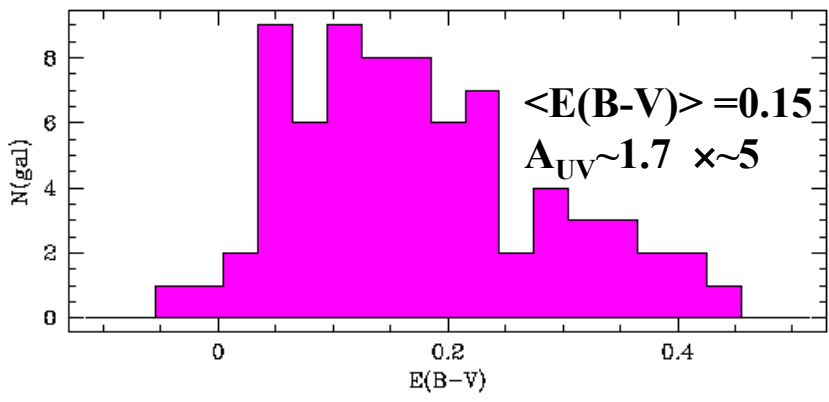
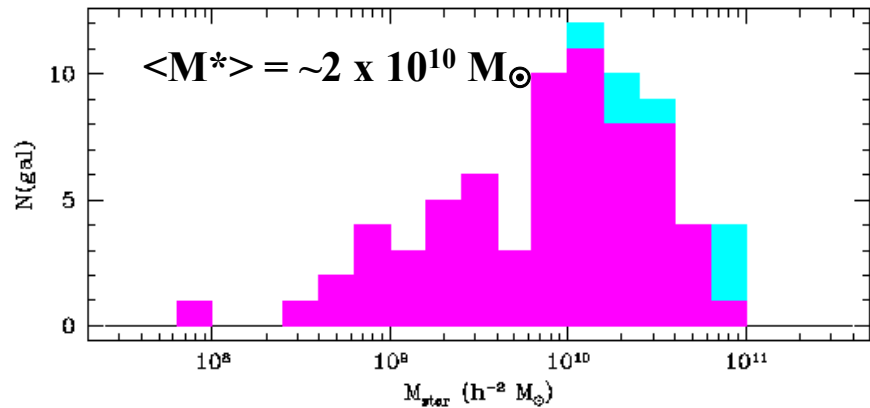
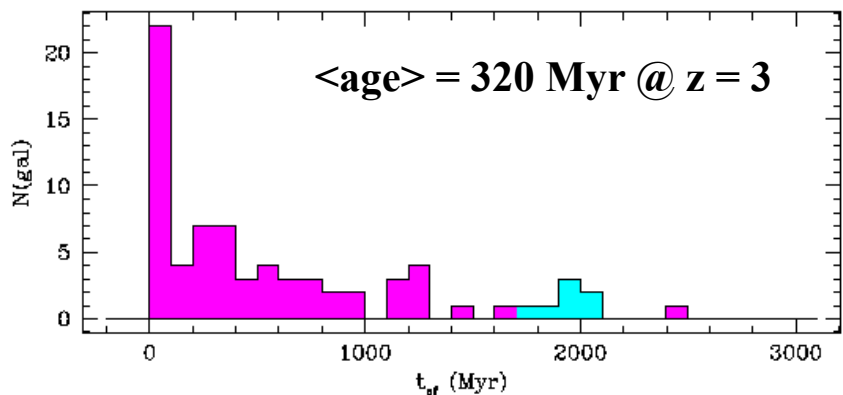
Spectral energy distributions allow us to predict where distant SF galaxies lie in color-color diagrams such as ($U-G$ vs $G-R$) (Steidel et al 1996)



Spectroscopic Confirmation at Keck



Properties of Lyman Break Galaxies (z~3)



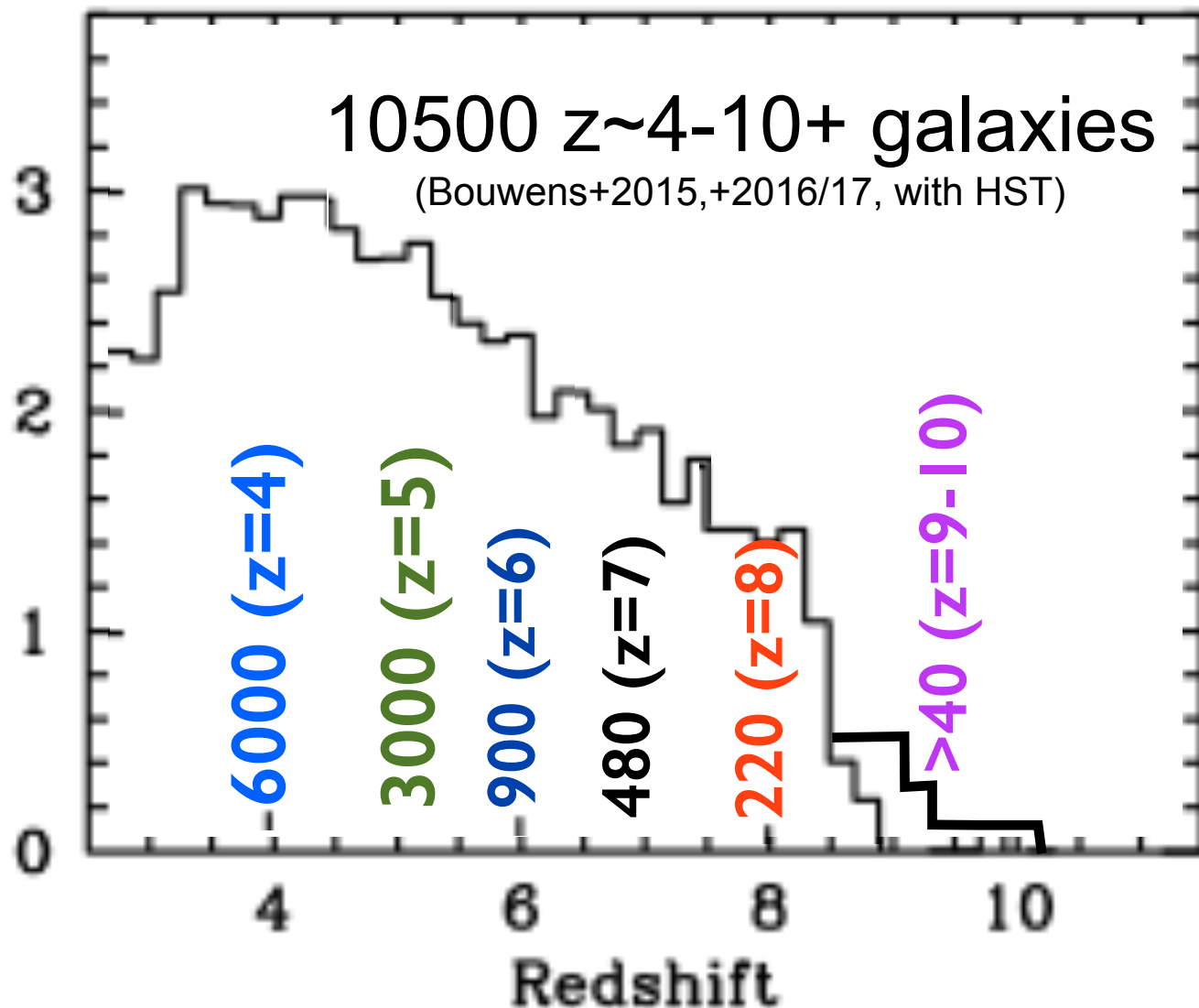
Extinction correlates with age— young galaxies are *much dustier*

SFR for youngest galaxies average $275 M_{\odot} \text{ yr}^{-1}$; oldest average $30 M_{\odot} \text{ yr}^{-1}$

Objects with the highest SFRs are the dustiest objects

Shapley et al 2001 Ap J 562, 95

Etat des lieux

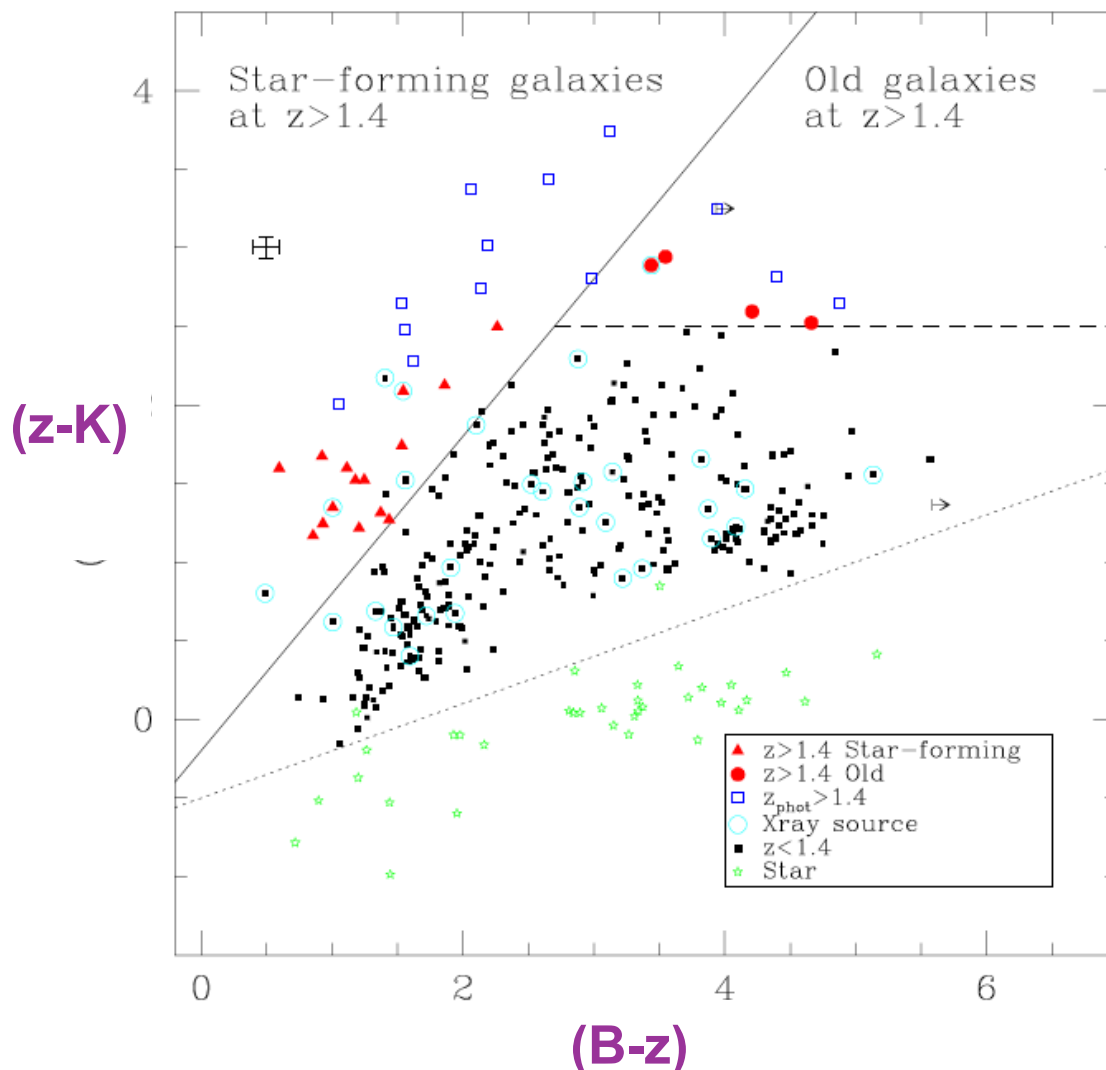


'BzK' selection of passive and SF $z>1.4$ galaxies

New apparently less-biased technique for finding *all* galaxies $1.4 < z < 2.5$

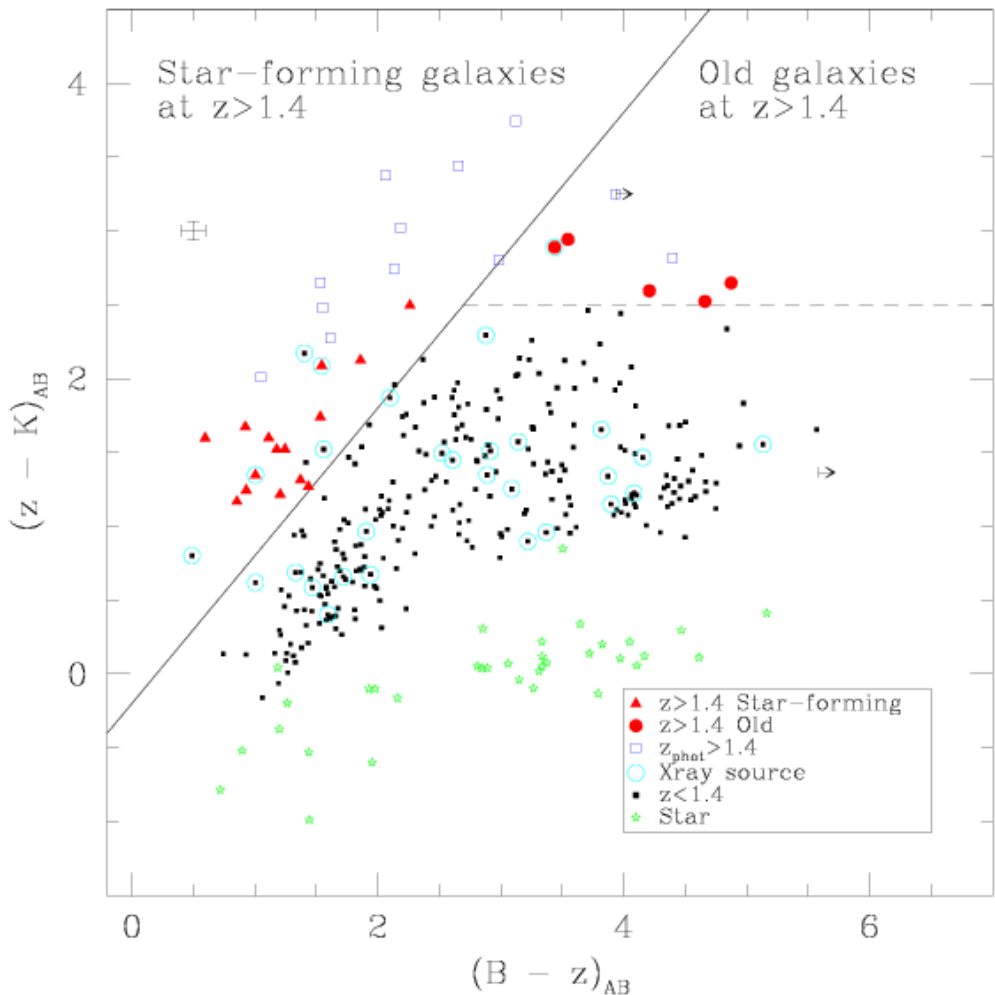
sBzK: star forming galaxies

pBzK: passive galaxies



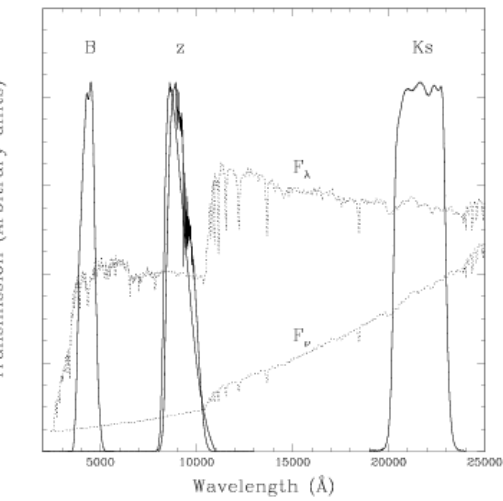
Daddi et al 2004 Ap J 617, 746

BzK selection technique:
 selection of $z \sim 2$ galaxies & separation of SF vs passive gals
 4000Å break for old stars, slope of continuum for young stars



$$\text{BzK} = (z - K) - (B - z) \text{ (AB mags)}$$

$\text{BzK} > -0.2 \rightarrow \text{SF at } z > 1.4$
 $\text{BzK} < -0.2 \text{ & } z - K > 2.5 \rightarrow \text{Old}$

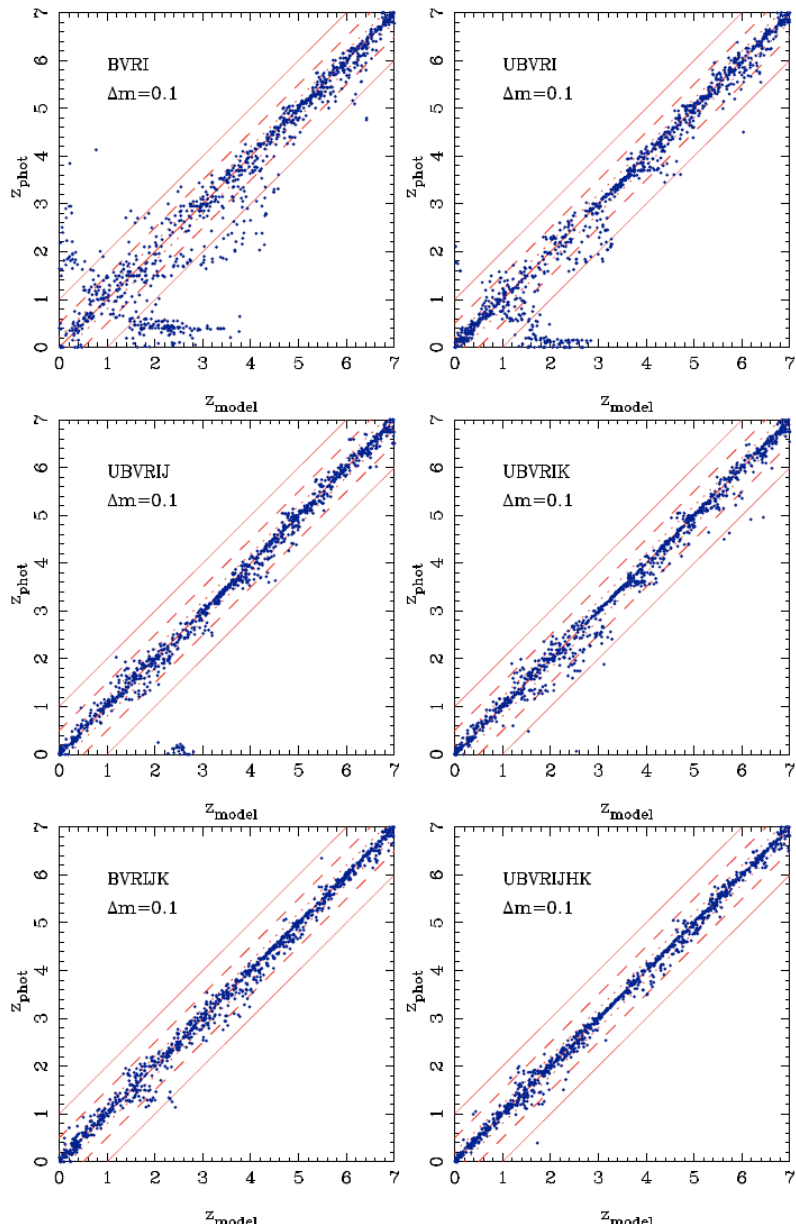


Daddi et al. 2005

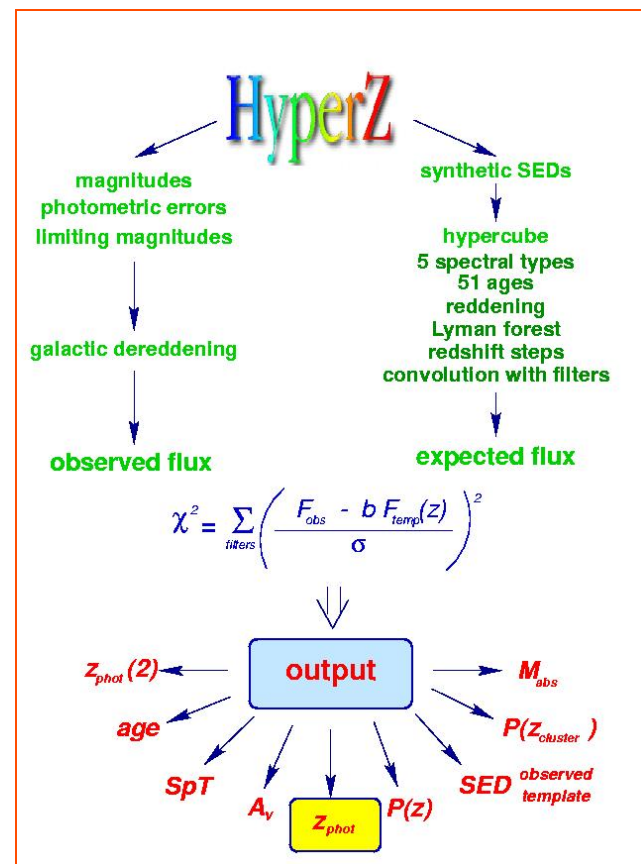
94% of spec redshifts; K20 survey

Technique calibrated with ~ 50 $z > 1.4$ redshifts

Les redshifts photométriques

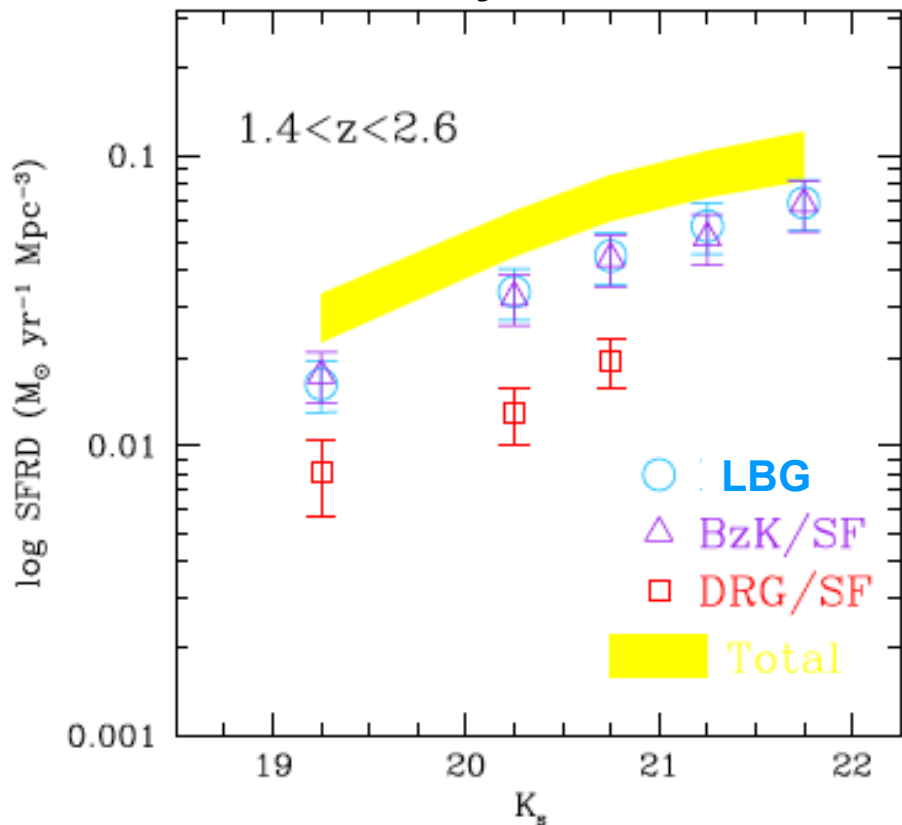


D'une manière plus générale, on utilise les discontinuités de Balmer et de Lyman pour obtenir une estimation du redshift des galaxies faibles, et donc difficiles d'accès en spectroscopie, à l'aide des leurs magnitudes en bandes larges. Plusieurs programmes sont accessibles pour réaliser ces calculs, dont HyperZ (Bolzonella, Miralles, Perro, 2000, <http://webast.ast.obs-mip.fr/hyperz>)



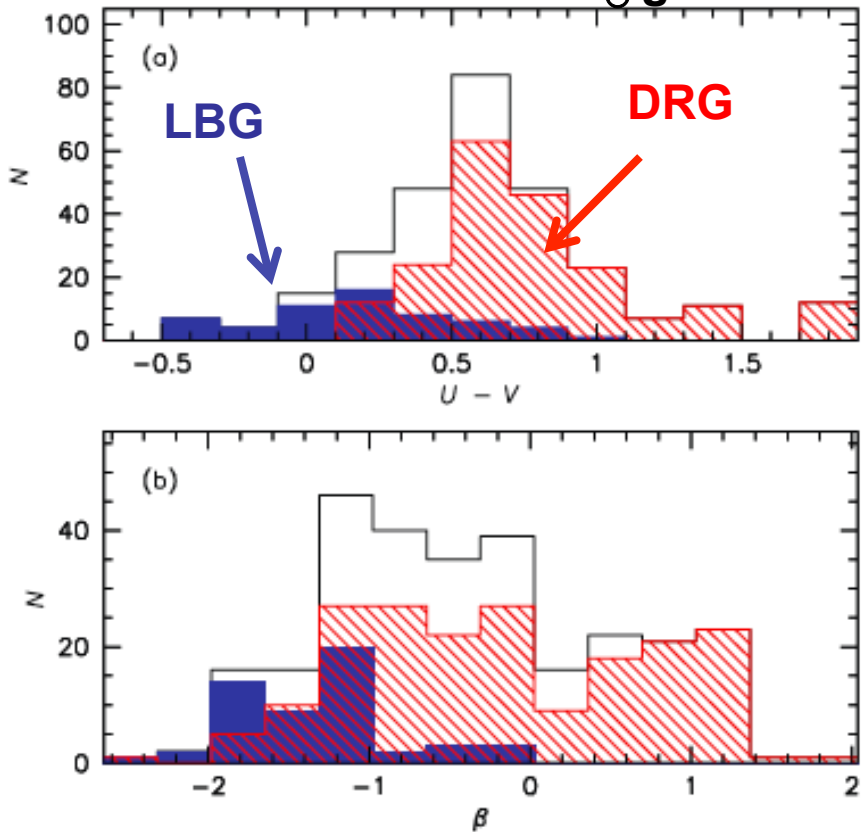
Connecting the BzK, LBG and DRG Populations

SF Density Contributions



Reddy et al 2005 Ap J 633, 248

Distribution of $M > 10^{11} M_\odot$ galaxies



van Dokkum et al 2006 Ap J 638, L59

van Dokkum et al (2006) - LBGs constitute only 17% of massive galaxies!

High-redshift galaxies in the *Hubble Deep Field*: colour selection and star formation history to $z \sim 4$

Piero Madau,^{1★} Henry C. Ferguson,^{1★} Mark E. Dickinson,^{1★} Mauro Giavalisco,^{2★†}
 Charles C. Steidel^{3★‡§} and Andrew Fruchter^{1★}

Absorption intergalactique

2 INTERGALACTIC ATTENUATION

In this section we will briefly review the theory of the propagation of UV radiation through a clumpy universe, following Madau (1995).

2.1 Basic equations

Let $L(\nu_{\text{em}})$ be the specific power emitted with frequency ν_{em} by a source at redshift z_{em} . The mean specific flux observed at Earth is

$$\langle f(\nu_{\text{obs}}) \rangle = \frac{(1+z_{\text{em}})L(\nu_{\text{em}})}{4\pi d_L^2} \langle e^{-\tau} \rangle, \quad (1)$$

where $\nu_{\text{obs}} = \nu_{\text{em}}/(1+z_{\text{em}})$, d_L is the luminosity distance to z_{em} and the average transmission over all lines of sight is, assuming Poisson-distributed clouds,

$$\langle e^{-\tau} \rangle = \exp \left\{ \int_0^{z_{\text{em}}} \int \frac{\partial^2 N}{\partial N_{\text{H}_1} \partial z} [1 - e^{-\tau_c}] dN_{\text{H}_1} dz \right\}. \quad (2)$$

Here, τ_c is the optical depth through an individual cloud at frequency $\nu = \nu_{\text{obs}}(1+z)$, and $(\partial^2 N / \partial N_{\text{H}_1} \partial z)$ is the redshift and column density distribution of absorbers along the path. An ‘effective’ optical depth of a clumpy medium can be defined as $\tau_{\text{eff}} = -\ln(\langle e^{-\tau} \rangle)$.

Along with resonant line scattering from Ly α , β , γ and higher order members, we include photoelectric absorption from H $_1$ in the Ly α forest clouds and Lyman limit systems along the line of sight. Since the bluest filter used for the *HDF* observations is centred at 3000 Å and has FWHM ~ 800 Å, galaxies will only be subject to H $_1$ cosmological attenuation from material located at $z \gtrsim (2600/1216) - 1 = 1.1$.

Lyman break selection

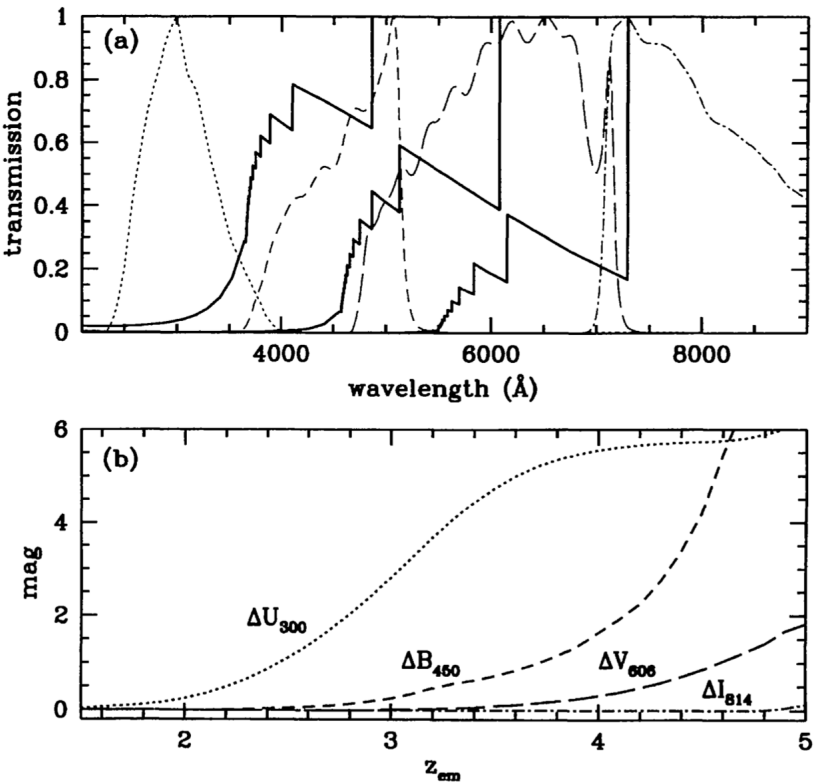
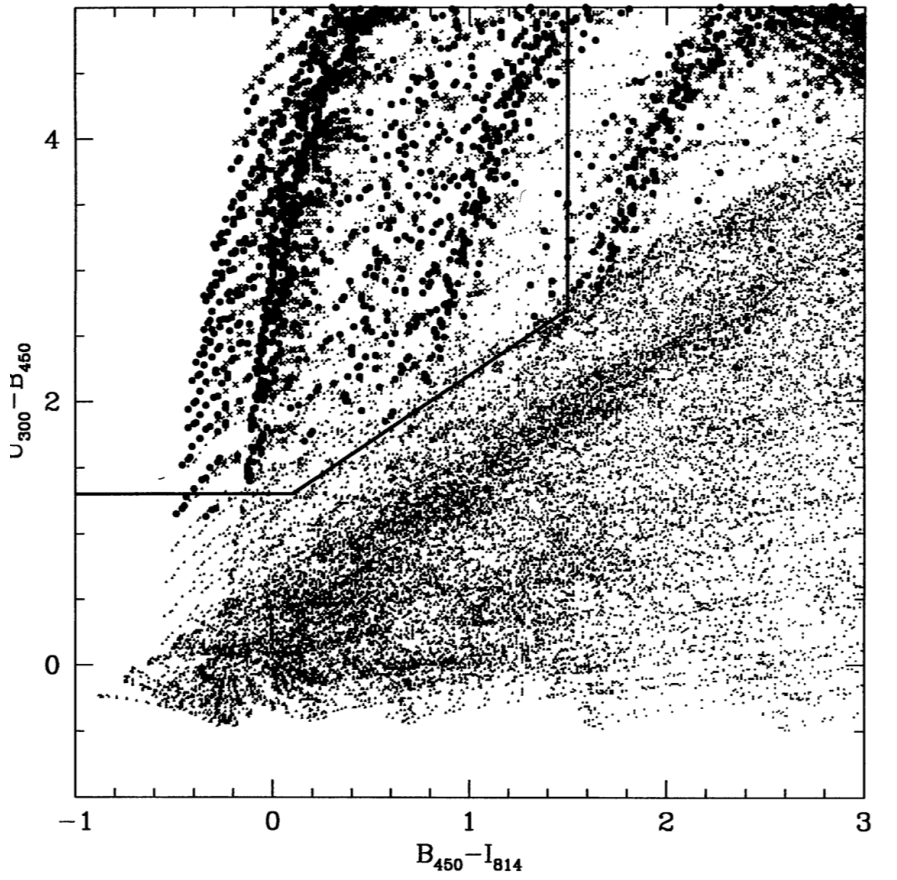


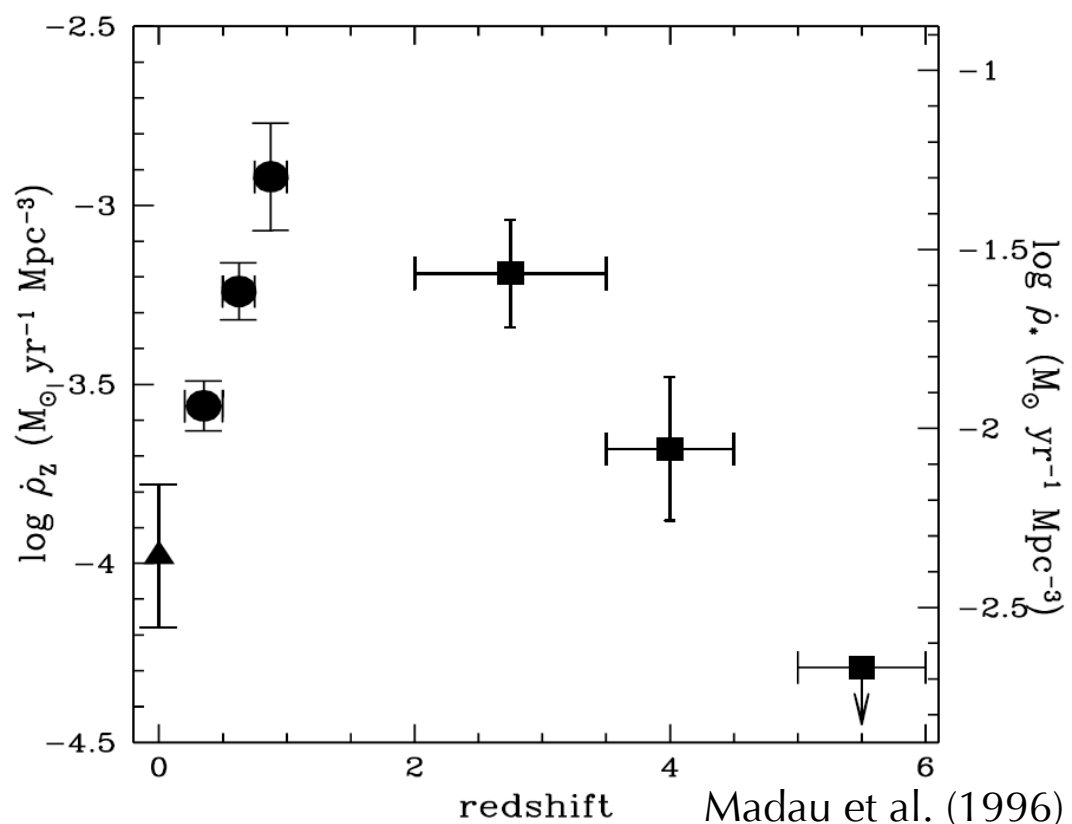
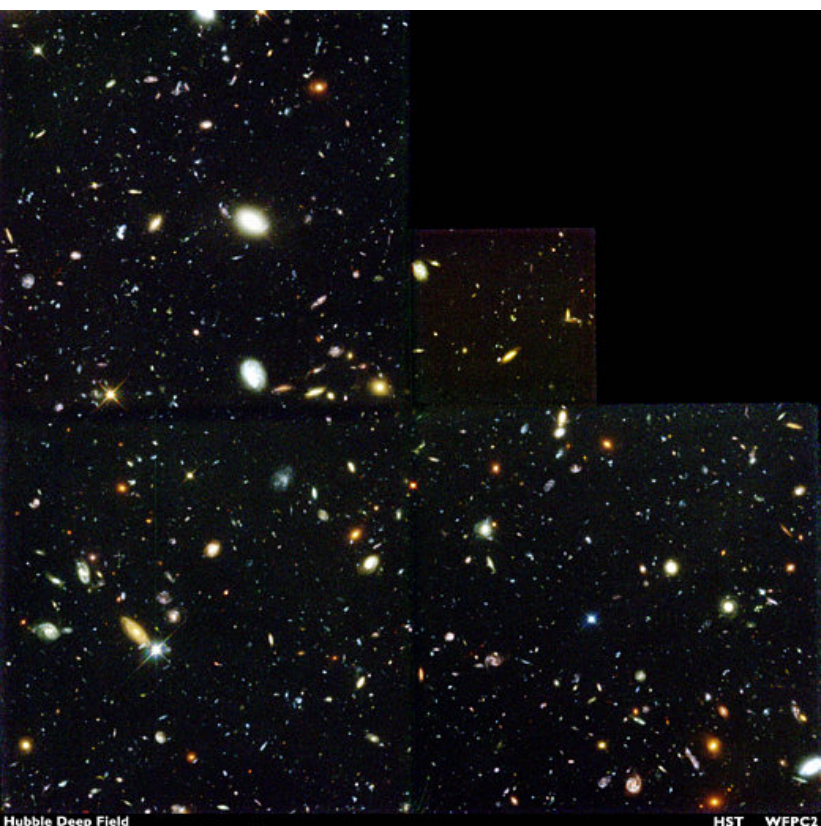
Figure 1. (a) Mean cosmic transmission for a source at $z_{em}=3, 4$ and 5 (solid lines), as a function of observed wavelength. The characteristic staircase profile is due to continuum blanketing from the Lyman series. Also plotted are the response functions of the four broad passbands, F300W (dotted line), F450W (short-dashed line), F606W (long-dashed line) and F814W (dash-dotted line) used for the *Hubble Deep Field*. (b) Magnitude increments ΔU_{300} (dotted line), ΔB_{450} (short-dashed lines), ΔV_{606} (long-dashed line) and ΔI_{814} (dash-dotted line), derived by integrating the mean cosmic transmission over the corresponding bandpass, as a function of the emission redshift.



$B_{450} - I_{814}$ for model galaxies. A total of 103 879 synthetic spectra of galaxies representing a wide range of metallicities, dust contents and redshifts were folded through the *HDF* bandpasses. The galaxies shown have redshifts less than 2 or redshifts of greater than 3.5. Galaxies shown as solid circles are those in the redshift range 2 < $z < 3.5$ and extinctions $A_B < 1$. \times s are galaxies in the same redshift range that have ages greater than 10^8 yr or extinctions $A_B > 1$. The selection criteria are $U_{300} - B_{450} > 1.3$, $U_{300} - B_{450} > B_{450} - I_{814} + 1.2$, and $B_{450} - I_{814} < 1.3$.

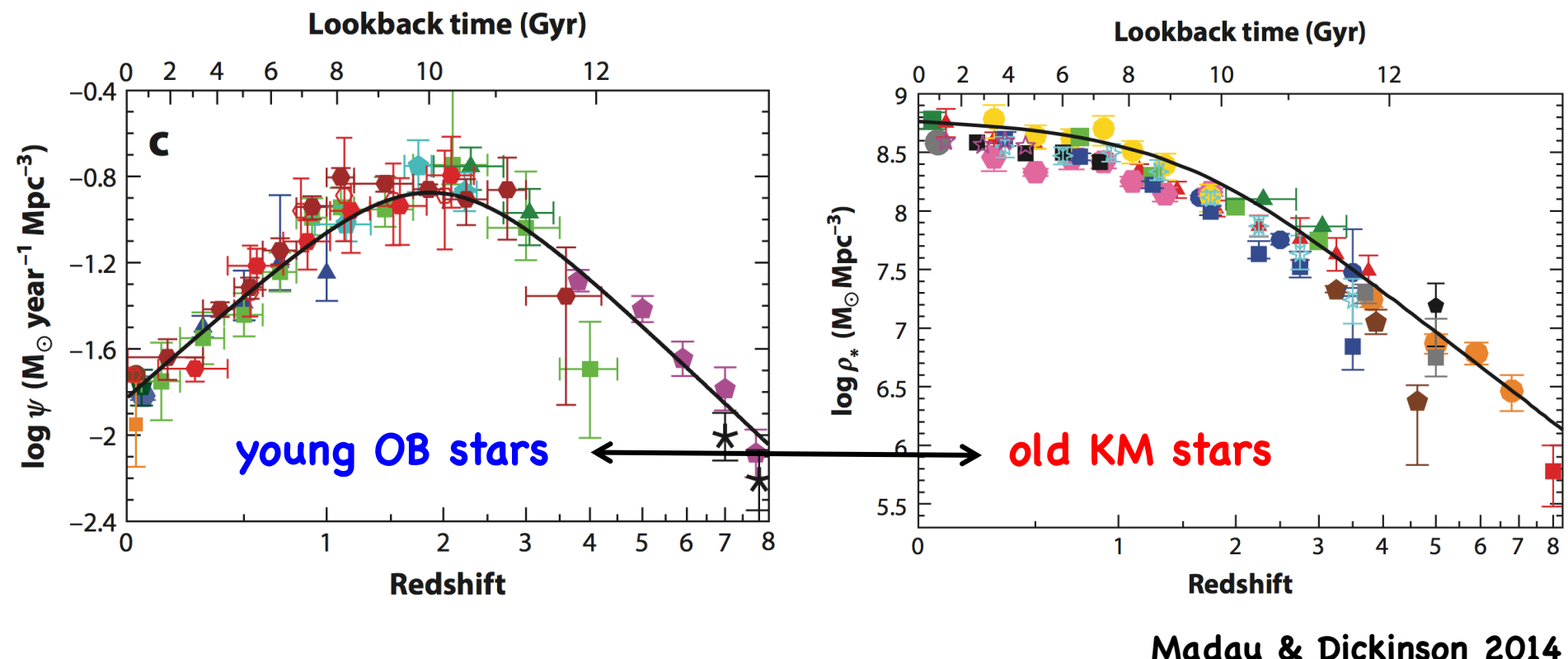
Histoire cosmologique de la formation d'étoiles

La densité de luminosité UV se mesure en $L_{\odot} \text{Mpc}^{-3}$, elle peut être traduite en terme de densité de formation d'étoiles en $M_{\odot} \text{yr}^{-1} \text{Mpc}^{-3}$, en utilisant le coefficient de conversion $L(\text{UV}) \rightarrow \text{SFR}$ de Kennicutt (1998). Mais il ne s'agit que d'une limite inférieure pour deux raisons: (i) on ne détecte que les galaxies les plus lumineuses, (ii) une fraction importante de la luminosité UV intrinsèque des étoiles d'une galaxie est absorbée par la poussière et réémise dans l'IR. En utilisant les LBG du HDFN (Hubble Deep Field Nord, image la plus profonde du ciel, jusqu'à une magnitude de 29), Madau et al. (1996) ont dérivé la première histoire cosmique de la formation d'étoiles, appelée "Madau plot", d'après une étude de la densité de $L(\text{UV})$ par Lilly et al. (1996).



cosmic SFR & M* density vs time

Une fois ces effets pris en compte, les données observationnelles deviennent plus cohérentes.



Constraints on models

- Stellar mass function
- Baryonic mass function
- HI mass function
- Luminosity function (in \neq bands)
- Cosmic SFR density
- Gas fractions
- Gas metallicities
- Stellar ages and metallicities
- SFR - M^* relation
- M_*/M_{halo} (from lensing)
- Black hole - bulge mass relation
- Tully - Fisher relation (L-v)
- Galaxy sizes
- Galaxy morphology
- Clusters: Hot gas (X-ray) vs total mass
- AGN bolometric luminosity function
- AGN mechanical luminosity function